Duan, Ruifeng; Zheng, Zhong; Jäntti, Riku; Hämäläinen, Jyri; Haas, Zygmunt. J.

Asymptotic Analysis for Spectrum-sharing Systems with TAS/MRC Using Extreme Value Theory

Published in:
IEEE Access

DOI:
10.1109/ACCESS.2019.2943083

Published: 23/09/2019

Document Version
Publisher's PDF, also known as Version of record

IEEE Access
Multidisciplinary | Rapid Review | Open Access Journal

Received July 31, 2019, accepted September 11, 2019, date of publication September 23, 2019, date of current version October 3, 2019.

Digital Object Identifier 10.1109/ACCESS.2019.2943083

Asymptotic Analysis for Spectrum-Sharing Systems With TAS/MRC Using Extreme Value Theory: An Overlooked Aspect

RUIFENG DUAN[1], (Member, IEEE), ZHONG ZHENG[2], (Member, IEEE), RIKU JÄNTTI[1], (Senior Member, IEEE), JYRI HÄMÄLÄINEN[1], (Senior Member, IEEE), AND ZYGMUNT J. HAAS[3,4], (Fellow, IEEE)

[1]Department of Communications and Networking, Aalto University, 02150 Espoo, Finland
[2]School of Information and Electronics, Beijing Institute of Technology, Beijing 100081, China
[3]Department of Computer Science, The University of Texas at Dallas, Richardson, TX 75080, USA
[4]School of Electrical and Computer Engineering, Cornell University, Ithaca, NY 14853, USA

Corresponding author: Zhong Zheng (zhong.zheng@bit.edu.cn)

The work of R. Duan and R. Jäntti was supported in part by the Business Finland through the Project 5G Finnish Open Research Collaboration Ecosystem (5G-FORCE). The work of Z. Zheng was supported in part by the Beijing Institute of Technology Research Fund Program for Young Scholars. This work of J. Hämäläinen was supported in part by the Academy of Finland under Grant 287249 and Grant 311752. The work of Z. J. Haas was supported in part by the Army Research Laboratory (ARL) under Contract W911NF-18-1-0406, and in part by the National Science Foundation (NSF) under Grant CNS-1763627.

ABSTRACT We investigate the asymptotic behavior for an overlooked aspect of spectrum-sharing systems when the number of transmit antennas n_t at the secondary transmitter (ST) grows to infinity. Considering imperfect channel state information (CSI), we apply the transmit antenna selection and the maximal-ratio combining techniques at the ST and the secondary receiver (SR), respectively. First, we obtain the signal-to-noise ratio (SNR) distributions received by the SR under perfect and imperfect CSI conditions. Then we show that the SNR distributions are tail-equivalent in the sense that the right tails of the two distributions decay in the same rate as the number of transmit antennas n_t grows to infinity. Based on the extreme value theory, when the transmit power of the ST is solely limited by the interference constraint, we show that the limiting SNR at the SR is Fréchet-distributed and the limiting rate scales as $\log(n_t)$. When the transmit power of ST is determined by both the maximal transmit power and the interference power constraints, the limiting SNR is Gumbel-distributed and the limiting rate scales as $\log(\log(n_t))$. We further show that the average rate can be estimated by the corresponding easier-to-obtain outage rate. Numerical results indicate that the derived asymptotic rate expressions represent accurate approximations even when n_t is ''not-so-large''. Finally, we study the robustness of the secondary transmissions by analyzing the corresponding average symbol error rates (SER) under general modulation and coding schemes. The findings indicate that the SER is Weibull distributed, when the maximal transmit power and interference power constraints are comparable.

INDEX TERMS Spectrum sharing, extreme value theory, rate scaling law, symbol error rate.

I. INTRODUCTION

Spectrum sharing has been considered as a promising technology to efficiently utilize the radio spectrum, and significant progress has been achieved in developing spectrum-sharing techniques, for instance, dynamic spectrum access and 5G heterogeneous networks [1], [2], licensed and unlicensed spectrum access [3], [4], drone networks [5], and co-primary spectrum sharing with applications in device-to-device communication [6]. In this work, we consider the underlay paradigm that the secondary users (SUs) operate as underlay systems. Therein, the SUs are allowed to coexist with the primary users (PUs)[1] while the SUs need to control

The associate editor coordinating the review of this manuscript and approving it for publication was Oussama Habachi.

[1]Although we call the communicating entities as SU and PU, the analysis in this paper can be applied in other communication systems that require interference control for transmission.

their transmit power in order to avoid harmful interference to the PUs [2], [7], [8]. The performance of such spectrum-sharing systems have been considered in literature, such as [2], [7], [8] among others.

It is well-known that the multi-antenna techniques can be used to improve the link-level performance of wireless communications. The transmitter antenna selection (TAS) scheme, among other transceiver designs, significantly reduces the hardware complexity and costs by simplifying the radio transmission units, as only a single RF chain is needed at the transmitter. In addition, the TAS scheme does not require synchronization among transmit antennas. Hence, it is an effective transceiver design and has been adopted in massive MIMO systems as well as the recent non-orthogonal multiple access systems [9]–[11]. Compared to other channel-dependent transmission schemes, TAS also reduces the required channel feedbacks [12], as only a single index of the transmit antenna to be activated is needed from the receiver to the transmitter. Moreover, TAS technique has been adopted in [13] to improve the robustness of massive MIMO systems against passive eavesdropping.

A combined TAS and receiver maximal ratio combining (MRC) scheme is analyzed in [14] in the traditional point-to-point communication systems. Therein, authors investigated the system performance in terms of the average bit-error rate, and showed that the maximal diversity order is equal to the product of the number of transmit and receive antennas. In [15] and [16], authors investigated the outage probability and the bit error rate of TAS/MRC for point-to-point communications in Rayleigh and Nakagami-m fading channels, respectively. Finally, in [17] authors deduce the expressions for the outage probability in a TAS/MRC system assuming multiple users with independent and identically distributed (i.i.d.) Nakagami-m channels. The full diversity benefit is achieved at a relatively high SNR level.

A. RELATED WORKS

The ergodic capacity of the SU with TAS at the secondary transmitter (ST) and MRC at the secondary receiver (SR) is investigated in [18] when there is no maximal transmit power constraint for the ST. In [19], on the other hand, the capacity-scaling law and diversity order for a cognitive radio system with MRC receiver is investigated. Therein, the asymptotic analysis is conducted in the high SNR regime without TAS. Furthermore, authors in [20] analyze the multiuser diversity gain for single-antenna overlaid cognitive radio systems. We note that in [20] the interference towards the primary receiver (PR) is avoided by the spectrum sensing and only the maximum transmit power constraint is activated at the transmitting ST.

When the instantaneous perfect channel state information (CSI) of both ST-to-PR and ST-to-SR links are available at the ST, authors in [21] present a closed-form expression for the cumulative distribution function (c.d.f.) of the secondary SNR applying the antenna selection, where the selection criterion is based on the ratio between channel gains of the ST-to-SR and ST-to-PR links. This c.d.f. is applied to obtain, for instance, the outage probability, ergodic capacity, and bit error probability (BEP). Though a simple expression is provided for high SNR regime, the general expression for the BEP consists of the parabolic cylinder function. In addition, the approximated expression of the ergodic capacity includes the Laguerre polynomials, which do not explicitly display the relation between the considered performance metrics and the number of transmit antennas. Moreover, as the number of transmit antennas grows, it is challenging for the secondary receiver to feedback the full CSI of the ST-to-SR link to the ST. In addition, TAS/MRC has been studied for underlay spectrum sharing in [22], where asymptotic expressions of outage probability have been obtained as the transmit power of the SU goes to infinity. This scenario can be deemed as a special case of the study in this work.

Authors in [23]–[25] have studied the impacts of the feedback delay and the co-channel interference on the performance of the considered systems for multi-user multiple amplify-and-forward (AF) relaying networks and spectrum-sharing relaying networks. Results in [23] show that the perfect feedback is required to achieve the full diversity order of the multi-user multiple AF relaying networks. The TAS/MRC approach has also been considered in [24] for spectrum-sharing relaying networks. Therein, the exact and approximate expressions for the outage probability of the secondary network are obtained, which shows that interference power constraint is closely related to the achievable diversity order and coding gain. Authors in [25] have considered a transmit beamforming and MRC-enabled AF relaying system with feedback delay and co-channel interference. Particularly, the exact expressions for the c.d.f. of the SINR and the upper and lower bounds of the ergodic capacity have been obtained. In [26], performance analysis of several TAS schemes has been conducted for an energy harvesting decode-and-forward relaying network, where the asymptotic outage probabilities have been obtained in high SNR regimes.

The previous works either provide complicated expressions for the performance metrics of the secondary systems or conduct the performance analysis in high SNR regime, when the perfect CSI of the communication channels are accessible. However, it is not a practical scenario for the secondary users to operate in the high SNR regimes with error-free channel estimations. In this work, we carry out the performance analysis of the secondary users at generic SNR levels under imperfect CSI at the secondary receivers, which has been overlooked in literature. Furthermore, based on the existing results, it is difficult to gain insight into the interplay between the transmit power and interference power constraints of the secondary users and their impacts on the performance of the considered TAS technique. For instance, for a moderate SNR value, how the two constraints directly affect the performance of the SU in terms of average rate, outage rate, and average symbol error rate as the number of transmit antennas increases.

Note that when the interference power constraint is not imposed, the limiting SNR distribution follows Gumbel distribution [27]. However, to the best of our knowledge, when both the transmit power and the interference power constraints are active, the limiting SNR distribution and the corresponding asymptotic performance metrics of the TAS/MRC secondary systems, as functions of the number of transmit antennas, are unknown and are non-trivial to deduce such results on the existing works. In particular, we show in this work that *the additional interference power constraint does change the limiting SNR distribution*.

B. CONTRIBUTIONS AND PAPER ORGANIZATION

To address the above discussed issues, at generic SNR levels, the extreme value theory (EVT) is applied to analyze various performance metrics of the secondary spectrum-sharing systems subject to both the maximal transmit power constraint at ST and the maximal interference power constraint at PR. The performance of such secondary system is evaluated via closed-form expressions for the limiting SNR distributions, the average rate, the outage rate, and the average symbol error rate (ASER) using general modulation and coding schemes. Based on these results, the scaling laws of the SU average rate and outage rate with respect to the number of transmit antennas will be derived. We summarize the contributions of this work as follows:

- Before applying TAS, the SNR distributions received by the secondary receiver are obtained under perfect and imperfect CSI conditions. In both cases, the SNR distributions are shown to be tail-equivalent in the sense that the right tails of the two distributions decay in the same rate as the number of transmit antennas n_t grows to infinity. Therefore, under both perfect and imperfect CSI conditions, the limiting SNR distribution after applying TAS can be obtained by using the same analytical framework of EVT, which facilitates the following performance analysis.
- The limiting SNR distribution of the SU converges to the Fréchet distribution when the maximal transmit power constraint dominates over the interference power constraint, which is hereafter referred to as the interference power limited regime (IPLR); otherwise, the limiting SNR distribution converges to the Gumbel distribution, which is referred to as the non-dominant regime (NDR).
- The average rate scales as $\log(n_t)$ in IPLR, while scales as $\log(\log(n_t))$ in NDR, as n_t increases. For large n_t, in IPLR there is a non-zero gap between the outage rate and the average rate, while in NDR the gap is vanishing as $\log(1 + 1/\log n_t)$. We show that the average rate can be estimated by the corresponding easier-to-obtain outage rate.
- The SER follows the Weibull distribution for general modulation and coding schemes with large n_t. Based on this result, a compact expression for the ASER is deduced.

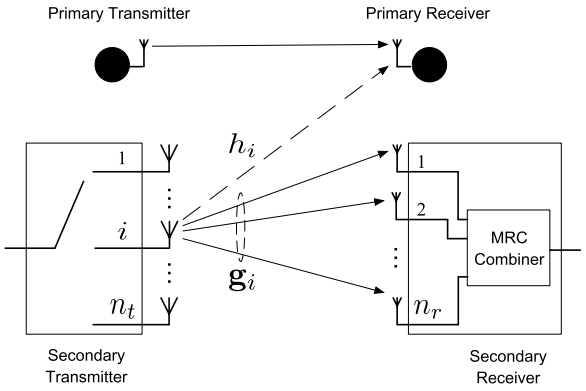

FIGURE 1. System Model: The *i*th antenna of the ST is selected.

The rest of the paper is organized as follows. In Section II, we outline the system model and present the c.d.f. of the SNR at the secondary receiver. In Section III, we briefly summarize the principles of the EVT, and derive the limiting distribution of the SNR at the secondary receiver. Using this result, the SU average rate and the corresponding rate scaling laws are investigated in Section IV. The SU outage rate is analysed in Section V. The average symbol error rate of the SU for general modulation types is deduced in Section VI. We present the simulation results in Section VII. Section VIII concludes this paper. Proofs of key technical results are provided in the Appendices.

C. NOTATIONS

We adopt the following notations: Q denotes instantaneous interference power constraint at the PR; P_m is the maximum transmit power constraint at the ST; $\mathbf{g}_i \in \mathbb{C}^{1\times n_r}$ represents the channel vector between the ith antenna of the ST and the antenna array of the SR; $h_i \in \mathbb{C}$ is the channel between the ith antenna element of the ST and the PR; $\mathbf{I}_n$ denotes $n \times n$ identity matrix; $\gamma(a,x) = \int_0^x t^{a-1}e^{-t}\,\mathrm{d}t$ and $\Gamma(a,x) = \int_x^\infty t^{a-1}e^{-t}\,\mathrm{d}t$ denote the lower and the upper incomplete Gamma function, respectively; $\gamma_0 = 0.5772\ldots$ is the Euler-Mascheroni constant; The error function and complementary error function are denoted as $\mathrm{erf}(x) = \frac{2}{\sqrt{\pi}}\int_0^x e^{-t^2}\,\mathrm{d}t$ and $\mathrm{erfc}(x) = 1 - \mathrm{erf}(x)$, respectively.

II. SYSTEM MODEL

Consider a spectrum-sharing system as shown in Fig. 1, which consists of a SU pair and a PU pair. The ST is equipped with n_t antenna elements, assuming that the transmit antenna selection is adopted. The secondary receiver (SR) has n_r antenna elements, and the received signals are combined according to the MRC principle. The primary transmitter (PT) and receiver (PR) are assumed to be equipped with one antenna.[2] To protect the PU communications, we consider an interference power constraint imposed by the PR, where the instantaneous interference from the ST to the PR is

[2]This corresponds to the legacy wireless systems, where the transceivers have limited hardware capability.

constrained within a pre-specified power threshold due to the radio regulations. Meanwhile, the transmit power of the ST is also limited by its maximum power constraint due to, for instance, hardware limitations or by spectrum access policies set by the regulators.

A. SIGNAL MODEL

When the ith transmit antenna of ST is used, the received signal vector at the SR, $\mathbf{y}$, reads

$$\mathbf{y} = \sqrt{\mu_g P_s^{(i)}}\,\mathbf{g}_i\, x + \mathbf{v}, \tag{1}$$

where μ_g denotes the average path loss between the transmit antennas and the receive antennas, and $P_s^{(i)}$ denotes the transmit power of the ST. Here, x is the transmitted symbol of ST, $\mathbf{g}_i$ is the channel vector whose elements $g_{i,j} \sim \mathcal{CN}(0,1)$, $j = 1, \cdots, n_r$, represent the complex channel coefficient between the ith transmit antenna and the jth receive antenna, and $\mathbf{v} \sim \mathcal{CN}(0, \sigma^2 \mathbf{I}_{n_r})$ is the complex white Gaussian noise vector. The channel vectors are i.i.d. standard complex Gaussian distributed, independent across transmit antennas. In this model, we adopt the same assumption for underlay spectrum sharing paradigm as in [7], [21], [28]–[31] that the interference from the PT is treated as Gaussian noise or via proper cooperative schemes [32] such that we can obtain analytic results with sufficient insights on the addressed problem. With multiple PTs, this can be justified by the central limit theorem and valid for certain network deployment topologies, for instance when the SR and the PT are far away [7], [31]. When the interference from the PU cannot be treated as Gaussian noise, the SR receives a combination of the signal, interference and noise, and the resulting SINRs of the received symbols sent by different transmit antennas become correlated. The following EVT analysis of such correlated random variables is an open problem in general. We leave this challenging problem for our future work. For the analysis, we have adopted the following assumptions on the signal model:

- (A1) The channels follow a block fading process, i.e., the entities of channel vectors remain constant over each coding block and are i.i.d across from one block to another;
- (A2) The SR has the imperfect CSI of $\mathbf{g}_i$, namely $\hat{\mathbf{g}}_i$, to perform maximal ratio combining; the ST has the imperfect CSI of h_i, namely $\hat{h}_i$;
- (A3) The PT and ST apply Gaussian codebooks.

We note that $\hat{h}_i$ in (A2) can be obtained, when, for instance, the primary receiver feeds back the channel measurement of $\hat{h}_i$ to the secondary transmitter [33]. These assumptions are applied also in previous works, for instance, [33]–[37] among others.

We consider the following imperfect CSI model, which has been widely applied in literature, where the pilot and the signal are sent separately within a fading channel block, for instance, [23]–[25], [38]–[40] among others. The imperfect CSIs of $\mathbf{g}_i$ and h_i are due to the Gaussian estimation errors such that

$$\hat{\mathbf{g}}_i = \sigma_g \mathbf{g}_i + \sqrt{1-\sigma_g^2}\,\tilde{\mathbf{g}}_i, \tag{2}$$

$$\hat{h}_i = \sigma_h h_i + \sqrt{1-\sigma_h^2}\,\tilde{h}_i, \quad \forall i. \tag{3}$$

where $\tilde{\mathbf{g}}_i \sim \mathcal{CN}(0, \mathbf{I}_{n_r})$ and $\tilde{h}_i \sim \mathcal{CN}(0,1)$ are the normalized channel estimation errors of $\mathbf{g}_i$ and h_i, respectively. The terms $0 \le \sigma_g, \sigma_h \le 1$ denote correlations between the instantaneous channel coefficients and their estimations. When σ_g and σ_h are equal to 1, the channel estimation is perfect; on the other hand, when σ_g and σ_h are equal to 0, the channel estimations fail completely and the channels are unknown to the transmitter.

Due to the imperfect CSI $\hat{h}_i$, the ST cannot strictly satisfy the interference power constraint set by the PR. Therefore, we consider the outage probability model for the interference power [24], where, in addition to the maximum transmission power P_m of the ST, it causes an interference towards the PR no larger than the power $\bar{Q}$ with a pre-defined outage probability ν. That is, $\Pr\left\{\mu_h P_s^{(i)} |\hat{h}_i|^2 \le \bar{Q}\right\} = \nu$. Following [24], the transmit power of the ST is given by

$$P_s^{(i)} = \min\left\{\frac{\kappa \bar{Q}}{\mu_h\,|\hat{h}_i|^2}, P_m\right\},$$

where κ is a power margin, and μ_h denotes the average path loss between the ith ST antenna and the receive antenna of the PR. Given the outage probability ν, the power margin κ can be numerically obtained by using [24, Eq. (15)]. In this paper, we consider that κ is absorbed into $\bar{Q}$, i.e., $Q = \kappa \bar{Q}$, so that the transmission power of the ST becomes

$$P_s^{(i)} = \min\left\{\frac{Q}{\mu_h\,|\hat{h}_i|^2}, P_m\right\}. \tag{4}$$

By using MRC at the SR, the received signals at the SR antenna array are weighted by the corresponding complex channel coefficients and combined coherently [41]. The post-processed signal after the MRC at the SR can be written as

$$\tilde{y} = \mathbf{w}^\dagger \mathbf{y} = \sqrt{\mu_g P_s^{(i)}}\,\frac{\hat{\mathbf{g}}_i^\dagger}{||\hat{\mathbf{g}}_i||_F}\mathbf{g}_i\, x + \frac{\hat{\mathbf{g}}_i^\dagger}{||\hat{\mathbf{g}}_i||_F}\mathbf{v}, \tag{5}$$

where $\mathbf{w} = \frac{\hat{\mathbf{g}}_i}{||\hat{\mathbf{g}}_i||_F}$ is the MRC weight vector, $||\cdot||_F$ is the Frobenius norm, and $(\cdot)^\dagger$ denotes the complex conjugate transpose operator. Assuming perfect CSI first, the channel power gain $||\mathbf{g}_i||_F^2$ follows a Chi-square distribution with $2n_r$ degrees of freedom, and the c.d.f. of $||\mathbf{g}_i||_F^2$ is given by [42] as:

$$F_{||\mathbf{g}_i||_F^2}(x) = 1 - \frac{1}{(n_r-1)!}\Gamma\left(n_r, \frac{x}{\mu_g}\right), \quad x \ge 0. \tag{6}$$

With the imperfect CSI in (2), the c.d.f. of $||\hat{\mathbf{g}}_i||_F^2$ is given by [38], which has been applied in, e.g., [40], as:

$$F_{||\hat{\mathbf{g}}_i||_F^2}(x) = \sum_{m=1}^{n_r} B_{m-1}^{n_r-1}(\sigma_g^2)\left(1 - \frac{\Gamma\left(m, \frac{x}{\mu_g}\right)}{\Gamma(m)}\right), \tag{7}$$

where $B_i^k(t) = \binom{k}{i} t^i (1-t)^{k-i}$ denotes Bernstein basis polynomial of degree k with $\binom{k}{i}$ being a binomial coefficient.

The post-processed SNR corresponding to the ith antenna transmission at the MRC combiner of the SR is of the form

$$\hat{\gamma}_i = \min\left\{\frac{\mathrm{S}_Q\|\hat{\mathbf{g}}_i\|_F^2}{|\hat{h}_i|^2}, \mathrm{S}_P\|\hat{\mathbf{g}}_i\|_F^2\right\}. \tag{8}$$

where $\mathrm{S}_P = P_m/\sigma^2$, and $\mathrm{S}_Q = Q/\mu_h\sigma^2$. If TAS is applied at ST, its i^*th transmit antenna corresponding to the largest receive SNR $\hat{\gamma}_{i^*}$ is selected to transmit the signals. That is, the SR feedbacks the antenna index i^*, which fulfills

$$i^* = \arg\max_{1\le i\le n_t} \hat{\gamma}_i. \tag{9}$$

Assuming an ideal feedback channel between the ST and the SR, the TAS scheme requires $\log_2 n_t$ bits of feedback information. The largest SNR is denoted by $\gamma_{\max} = \max_{1\le i\le n_t} \hat{\gamma}_i$.

Proposition 1: The c.d.f. of the post-processed SNR $\hat{\gamma}_i$ with imperfect CSI is given as:

$$F_{\hat{\gamma}_i}(x) = \sum_{m=1}^{n_r} B_{m-1}^{n_r-1}(\sigma_g^2)\left\{1 - \frac{1}{\Gamma(m)}\left[\Gamma\left(m, \frac{x}{\mu_g \mathrm{S}_P}\right) - \left(\frac{x}{\mu_g \mathrm{S}_Q + x}\right)^m \Gamma\left(m, \frac{x}{\mu_g \mathrm{S}_P} + \frac{\mathrm{S}_Q}{\mathrm{S}_P}\right)\right]\right\}. \tag{10}$$

Proof: The proof of Proposition 1 is in Appendix A. ■

Note that by setting $\sigma_g^2 = 1$, the c.d.f. of γ_i in (11) is obtained from (10) as:

$$F_{\gamma_i}(x) = 1 - \frac{1}{\Gamma(n_r)}\left[\Gamma\left(n_r, \frac{x}{\mu_g \mathrm{S}_P}\right) - \left(\frac{x}{\mu_g \mathrm{S}_Q + x}\right)^{n_r} \Gamma\left(n_r, \frac{x}{\mu_g \mathrm{S}_P} + \frac{\mathrm{S}_Q}{\mathrm{S}_P}\right)\right], \tag{11}$$

which is in line with the existing results in [18] and [19]. Based on (9), the c.d.f. of $\gamma_{\max}$ can be expressed as [43]

$$F_{\gamma_{\max}}(x) = \left[F_{\hat{\gamma}_i}(x)\right]^{n_t}. \tag{12}$$

Considering a simplified scenario with $P_m \to \infty$ and hence $\mathrm{S}_P \to \infty$, the c.d.f. in (10) can be approximated, by applying $\Gamma(n_r, 0) = \Gamma(n_r)$ [50, eqn. (8.350-4)], as

$$F_{\hat{\gamma}_i}(x) = \sum_{m=1}^{n_r} B_{m-1}^{n_r-1}(\sigma_g^2)\left(\frac{x}{x + \mu_g \mathrm{S}_Q}\right)^m. \tag{13}$$

With perfect CSI at the ST, (13) can be reduced to

$$F_{\gamma_i}(x) = \left(\frac{x}{x + \mu_g \mathrm{S}_Q}\right)^{n_r}. \tag{14}$$

B. CONCEPT OF TAIL EQUIVALENCE

In this section, we prove that the limiting SNR distributions under the perfect and the imperfect CSI conditions are tail-equivalent so that the limiting behavior of the SNR $\gamma_{\max}$ remains the same as n_t grows. For the sake of completeness, the definition of tail equivalence in [44] is stated next.

Definition 1 (Tail Equivalence [44, Eq. (1.25)]): Let F and G be two distribution functions, and set their upper end-points as $\omega(F) = \sup\{y|F(y) < 1\}$ and $\omega(G) = \sup\{y|G(y) < 1\}$, respectively. Then F and G are (right) tail equivalent for some $\zeta > 0$ if, and only if, $\omega(F) = \omega(G)$ and

$$\lim_{x\to\omega(F)} \frac{1 - F(x)}{1 - G(x)} = \zeta. \tag{15}$$

In the next proposition, we show that the SNR distributions with and without channel estimation errors are tail-equivalent.

Proposition 2: The distribution functions $F_{\hat{\gamma}_i}(x)$ in (10) and $F_{\gamma_i}(x)$ in (11) are right tail equivalent and

$$\lim_{x\to\omega(F)} \frac{1 - F_{\hat{\gamma}_i}(x)}{1 - F_{\gamma_i}(x)} = \zeta \le (\sigma_g^2)^{n_r-1}. \tag{16}$$

Proof: The proof of Proposition 2 is in Appendix B. ■

Obviously, with the perfect CSI, i.e., $\sigma_g^2 = 1$, the ratio between the two tails is one as expected. In presence of imperfect CSI, the right-hand-side of (2) reduces as the accuracy of the channel estimation decreases, which means the receiver with imperfect CSI sees a degraded SNR compared to the case with perfect CSI. The SNR degradation is proportional to $(\sigma_g^2)^{n_r-1}$.

To the best of our knowledge, there is no explicit expressions for the performance metrics of the secondary users, such as the average rate and the average symbol error rate, obtained with the c.d.f. (10) or (12) due to their complexity. To enable a tractable analysis and gain insight into the considered cognitive radio system, we deduce the asymptotic expressions for the average rate, outage rate, and average symbol error rate using EVT by increasing the number of transmit antennas $n_t \to \infty$ while keeping the number of receive antennas n_r fixed.

III. EXTREME VALUE THEORY

The EVT provides elegant and powerful statistical tools when investigating the asymptotic distributions of the maximum or the minimum of a set of random variables [45]. Recently, EVT has proven useful in investigating the performance of the wireless communication networks. The authors in [46] conduct the asymptotic throughput analysis for the channel-aware scheduling in multi-user communications. The asymptotic antenna selection gain and the capacity distribution for a multi-antenna system are studied in [27] and the so-called cumulative distribution function based multi-user scheduling are investigated using EVT in [47] and [48]. Moreover, authors in [34] investigate a single-antenna spectrum-sharing multi-hop relay system, where the EVT is applied to obtain the limiting distribution functions of the lower and upper bounds on the end-to-end SNR of the relaying path.

A. PRELIMINARY

Let $X_1, X_2, \ldots, X_n$ denote a sequence of i.i.d. random variables with distribution $F_X(x)$ and $M_n = \max\{X_i : 1 \le i \le n\}$. Furthermore, assume that there exists sequences of real

numbers a_n and b_n such that

$$\lim_{n\to\infty} \frac{M_n - a_n}{b_n} \xrightarrow{d} \mathcal{G}, \tag{17}$$

where $\xrightarrow{d}$ denotes the convergence in distribution and $\mathcal{G}$ is a non-degenerate distribution. By the Fisher-Tippet-Gnedenko theorem [49] it is known that $\mathcal{G}$ is one of the extreme value distributions: Gumbel, Fréchet, or Weibull, defined as:

$$\text{Weibull: } \Psi_\xi(x) = e^{-(-x)^{-1/\xi}}, \quad x \le 0,\ \xi < 0 \tag{18a}$$

$$\text{Fréchet: } \Phi_\xi(x) = e^{-x^{-1/\xi}}, \quad x \ge 0,\ \xi > 0 \tag{18b}$$

$$\text{Gumbel: } \Lambda_\xi(x) = e^{-e^{-x}}, \quad x \in \mathbb{R},\ \xi = 0, \tag{18c}$$

where ξ denotes the extreme value index. Furthermore, according to the assumption (17), the distribution $F_X(x)$ belongs to the so-called Maximum Domain of Attraction (MDA) of $\mathcal{G}$.

This EVT result forms a basis of the asymptotic approximation for the SNR distribution (12) when the number of transmit antenna n_t is large. This asymptotic distribution relies on the MDA of the underlying distribution $F_X(x)$. As we show in the following discussions, the SNR distribution $F_{\gamma_i}(x)$ for the perfect CSI scenario in (11) belongs to the MDA of the Gumbel or the Fréchet distribution, depending on the dominating power constraints Q and P_m. Since the distribution functions $F_{\gamma_i}(x)$ and $F_{\hat{\gamma}_i}(x)$ are tail-equivalent as been shown in Section II-B, the SNR distribution $F_{\hat{\gamma}_i}(x)$ for the imperfect CSI scenario in (10) lies on the same MDA, where $F_{\gamma_i}(x)$ belongs [44]. Prior to using the extreme value distributions to approximate $F_{\gamma_{\max}}(x)$ in (12), we first review two relevant results from [45], which state the sufficient conditions for a distribution to belong to the MDA of the Gumbel and the Fréchet distributions.

Lemma 1 [45, Theorem 2.7.2]: Let $\omega(F_X) = \sup\{x : F_X(x) < 1\}$ as the right end-point of the support of $F_X(x)$. Assume that there is a real number x_1, and for $x_1 \le x < \omega(F_X)$, $f_X(x) = F_X'(x) \neq 0$ and $F_X''(x)$ exists. If

$$\lim_{x\to\omega(F_X)} \frac{d}{dx}\left[\frac{1 - F_X(x)}{f_X(x)}\right] = 0, \tag{19}$$

then $F_X(x)$ lies on the MDA of the Gumbel distribution with the c.d.f. expressed as

$$\Lambda_\xi(x) = \exp\left(-\exp\left(-\frac{x - a_n}{b_n}\right)\right), \tag{20}$$

with the normalizing coefficients a_n and b_n determined by

$$a_n = F_X^{-1}(1 - 1/N), \quad b_n = F_X^{-1}(1 - 1/Ne) - a_n. \tag{21}$$

Here e is the base of the natural logarithm, and $F_X^{-1}(\cdot)$ denotes the inverse of the distribution function.

A sufficient condition that a distribution lies on the MDA of the Fréchet distribution is given as follows:

Lemma 2 [45, Theorem 2.1.1]: Let $\omega(F_X) = \sup\{x : F_X(x) < 1\} = \infty$. Assume that there is a constant $\nu > 0$ such that the following limit exists for all $x > 0$,

$$\lim_{t\to\infty} \frac{1 - F_X(tx)}{1 - F_X(t)} = x^{-\nu}, \tag{22}$$

where $\nu = 1/\xi$. Then, $F_X(x)$ lies on the MDA of the Fréchet distribution with the c.d.f. expressed as

$$\Phi_\xi(x) = \exp\left[-\left(\frac{x}{b_n}\right)^{-1/\xi}\right], \quad \forall x > 0, \tag{23}$$

with the coefficients determined by

$$a_n = 0, \quad b_n = F_X^{-1}(1 - 1/N). \tag{24}$$

We note that the choice of the normalizing coefficients a_n and b_n are not unique, and they can be selected as in other forms without affecting the convergence of (17) to the limiting distributions (18) [45]. Nevertheless, we show in Section VII that the adopted normalizing coefficients (21) and (24) can be used to construst accurate approximations for the considered performance metrics when the number of antennas n_t is finite.

B. LIMITING SNR DISTRIBUTION OF THE SECONDARY USER

We categorize the operational regimes of the considered spectrum-sharing system into the following cases:

- Interference power limited regime (IPLR): $P_m \to \infty$ with Q/μ_h fixed.
- Transmit power limited regime (TPLR): $Q/\mu_h \to \infty$ with P_m fixed.
- Otherwise, non-dominant regime (NDR).

Note that the system in TPLR can be reduced to the one studied in [27]. We will, therefore, focus on the operational regimes IPLR and NDR. Using Lemma 1 and Lemma 2, we prove in the next propositions that the c.d.f. of the SNR $F_{\gamma_i}(\cdot)$ in (11) lies on the MDA of the Gumbel or Fréchet distributions for the two considered scenarios, i.e., IPLR and NDR, respectively. Recall that, as defined in the previous section, $\mathrm{S}_P = P_m/\sigma^2$, $\mathrm{S}_Q = Q/\mu_h\sigma^2$, and $\lim_{x\to\omega(F)} \frac{1-F_{\hat{\gamma}_i}(x)}{1-F_{\gamma_i}(x)} = \zeta \le (\sigma_g^2)^{n_r-1}$.

Proposition 3: Given the transmit power (4), the distribution $F_{\hat{\gamma}_i}(\cdot)$ in (10) lies on the MDA of the Fréchet distribution in IPLR, and the SNR distribution of TAS/MRC secondary user is given by

$$F_{\gamma_{\max}}(x) = \exp(-b_n/x), \quad \forall x > 0 \tag{25}$$

with the coefficient b_n chosen as

$$b_n = \frac{\mu_g \mathrm{S}_Q}{[n_t/(n_t-1)]^{\zeta/n_r} - 1}. \tag{26}$$

Proof: The proof of Proposition 3 is in Appendix C. ■

Proposition 4: Given the transmit power (4), the distribution $F_{\hat{\gamma}_i}(\cdot)$ in (10) lies on the MDA of the Gumbel distribution in NDR. The SNR distribution of the secondary user with TAS/MRC is given by

$$F_{\gamma_{\max}}(x) = \exp\left(-\exp\left(-\frac{x - a_n}{b_n}\right)\right), \quad \forall x > 0 \tag{27}$$

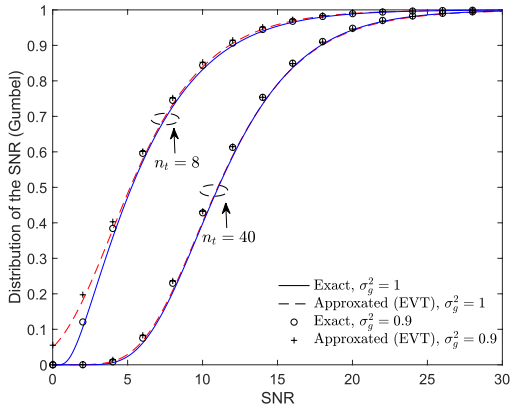

FIGURE 2. Exact and approximate distributions of the SU SNR when the best transmit antenna is selected in NDR (Gumbel), where $S_P = 5$dB and $S_Q = -5$dB. The number of receive antennas $n_r = 2$. The solid and dashed curves depict the exact and approximated distributions with perfect CSI, respectively. Markers '+' and 'o', respectively, denote the exact and approximated distributions with imperfect CSI, $\sigma_g^2 = 0.9$.

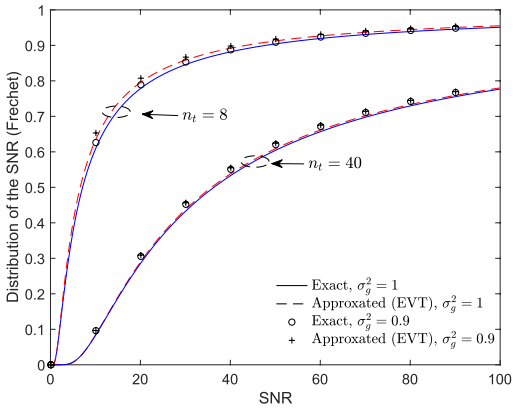

FIGURE 3. Exact and approximate distributions of the SU SNR when the best transmit antenna is selected in IPLR (Fréchet), where $S_P = 25$dB and $S_Q = -5$dB. The number of receive antennas $n_r = 2$. The solid and dashed curves depict the exact and approximated distributions with perfect CSI, respectively. Markers '+' and 'o', respectively, denote the exact and approximated distributions with imperfect CSI, $\sigma_g^2 = 0.9$.

where the coefficients a_n and b_n are

$$a_n = \mu_g \mathrm{S}_P \left[\log(n_t) + (n_r - 1)\log(\log(n_t)) - \log\Gamma(n_r) + \log(\zeta) + \log\left(1 - e^{-\mathrm{S}_Q/\mathrm{S}_P}\right)\right],$$
$$b_n = \mu_g \mathrm{S}_P. \tag{28}$$

Proof: The proof of Proposition 4 is in Appendix D. ■

Remark: In the considered spectrum-sharing cognitive radio system, the maximum transmit power P_m and the interference power constraint Q play significant roles in determining the limiting distribution of the SNR as $n_t \to \infty$, and thus, determining the asymptotic behavior of the secondary cognitive radio system. As the system operational regime shifts away from NDR, the limiting distribution transitions from the Gumbel distribution, in the form of double exponential function (18c), to the Fréchet distribution, in the form of single exponential function (18b). In other words, the dominance of the maximum transmit power determines the tail behavior of the SNR distribution, where the Fréchet distribution has a heavy tail and the Gumbel distribution has an exponential tail. Since the performance of the transmit antenna selection is determined by the tail behavior of the SNR distribution [27], Proposition 3 is vital to reveal the impact of the power constraints on the performance of the cognitive radio system. In Fig. 2 and Fig. 3, we compare the exact distributions (12) and the corresponding Gumbel and Fréchet distributions with perfect and imperfect CSI, respectively.

In the subsequent sections, we use Proposition 3 and Proposition 4 to obtain the scaling laws for the average rate and outage rate of the SU for the considered two scenarios, i.e. IPLR and NDR.

IV. ASYMPTOTIC AVERAGE RATE

For the considered secondary system with TAS/MRC configuration, the instantaneous rate of the SU in nats/s/Hz can be written as[3]

$$R_{\max} = \max_{1 \le i \le n_t} R_i, \tag{29}$$

where $R_i = \log\left(1 + \hat{\gamma}_i\right)$, $i = 1, \cdots, n_t$ is the instantaneous rate using the ith antenna. The average rate of SU can be obtained by averaging over the SNR distribution as

$$C = \int_0^\infty \log(1+\gamma)\, \mathrm{d}F_{\gamma_{\max}}(\gamma), \tag{30}$$

where the c.d.f. $F_{\gamma_{\max}}(\gamma) = \left[F_{\hat{\gamma}_i}(\gamma)\right]^{n_t}$ is given in (12) and $F_{\hat{\gamma}_i}(\gamma)$ is given in (10). To enable a tractable analysis for the average rate, we apply the asymptotic SNR distribution obtained in Section III. The obtained results represent the asymptotic performance of the considered system when the number of transmit antenna is large. However, numerical results in Section VII show that they serve as good approximations even for moderate number of transmit antennas. In addition, the asymptotic analysis enables insight into the rate scaling of the secondary user.

A. ASYMPTOTIC AVERAGE RATE IN IPLR

Replacing the limiting distribution in (23) into (30), the asymptotic SU average rate for large n_t can be obtained as

$$\begin{aligned} C_{\mathrm{IPLR}} &= \int_0^\infty \log(1+x)\mathrm{d}e^{-\left(\frac{x}{b_n}\right)^{-1}} \\ &= b_n\left[\int_0^\infty \log(1+t)e^{-tb_n}\mathrm{d}t - \int_0^\infty \log(t)e^{-tb_n}\mathrm{d}t\right] \\ &= \gamma_0 - e^{b_n}\mathrm{Ei}[-b_n] + \log(b_n), \end{aligned} \tag{31}$$

where b_n is given in (26), $\gamma_0 = 0.5772\ldots$ is the Euler-Mascheroni constant, $\mathrm{Ei}[w] = -\int_{-w}^{\infty} \frac{e^{-t}}{t}\, dt, \forall w < 0$ denotes the exponential integral function [50, Eq. (8.211)], the second

[3] In this paper, we use Shannon capacity to approximate the rate.

equality is obtained by applying substitution $t = 1/x$, and the third equality is obtained by applying [50, Eq. (4.331-1) and Eq. (4.337-2)]. Applying power series expansion for b_n in (26) as $n_t \to \infty$, we obtain

$$b_n = \left(n_t n_r - \frac{n_r + 1}{2}\right) \frac{\mu_g \mathrm{S}_Q}{\zeta} + O\left(\frac{1}{n_t}\right), \tag{32}$$

where the notation $f(x) = O(g(x))$ is defined as $\limsup_{x\to\infty} |f(x)/g(x)| < \infty$. Since $e^z \mathrm{Ei}[-z] \to 0$ as $z \to \infty$, the asymptotic, in n_t, average rate C_{IPLR} given in (31) can be approximated as

$$\widetilde{C}_{\mathrm{IPLR}} \approx \log(b_n) + \gamma_0 \propto \log(n_t n_r). \tag{33}$$

Remark: This result indicates that the average rate scales logarithmically with the product of n_t and n_r for large n_t. For fixed n_r, the scaling law in terms of n_t for the average rate is $\log(n_t)$. However, this explicit and simple results cannot be seen directly from [18, Eq. (12)].

In the next subsection, we consider another operational scenario of the spectrum sharing system, where the maximum power P_m of ST is comparable to the interference power constraint Q/μ_h, i.e., operation in the NDR regime.

B. ASYMPTOTIC AVERAGE RATE IN NDR

Based on Proposition 4, the SNR distribution of the secondary system in NDR lies on the MDA of Gumbel distribution. The corresponding average rate can be obtained by applying the limiting throughput theorem (LTD) from [46], which is listed as follows.

Lemma 3 [46]: Let Γ_i denote the received SNR at the secondary receiver when ith transmit antenna is used. Assume that Γ_i, $i = 1, \cdots, N$, are i.i.d. with a common distribution $F(\gamma)$ and the supremum $\omega(F(\gamma)) \to \infty$. The distribution of throughput lies on the MDA of the Gumbel distribution if the distribution of the SNR belongs to the MDA of the Gumbel distribution.

Due to Lemma 3, we have $\lim_{n_t\to\infty} (R_{\max} - \tilde{a}_n)/\tilde{b}_n \xrightarrow{d} \Lambda_\xi(x)$ and $\Lambda_\xi(x)$ is expressed in (20) with the following normalizing coefficients obtained by (21) as

$$\begin{aligned} \tilde{a}_n &= \log\left[1 + F_{\hat{\gamma}_i}^{-1}(1 - 1/n_t)\right], \\ \tilde{b}_n &= \log\left[1 + F_{\hat{\gamma}_{i_i}}^{-1}(1 - 1/n_t e)\right] - \tilde{a}_n. \end{aligned} \tag{34}$$

Using [46, Lemma 2], the expectation of $(R_{\max} - \tilde{a}_n)/\tilde{b}_n$ converges, and the average rate of the SU, $C = \mathbb{E}[R_{\max}]$, can be approximated by integrating $R_{\max}$ over (20) as

$$C_{\mathrm{NDR}} = \tilde{a}_n + \tilde{b}_n \gamma_0. \tag{35}$$

The approximation is tight in the asymptotic regime $n_t \to \infty$, since the approximation error is induced from Proposition 4. Observing the normalizing coefficients given in (34) for the limiting throughput distribution and the ones in (21) for the limiting SNR distribution (replacing N by n_t), we have $\tilde{a}_n = \log(1 + a_n)$ and $\tilde{b}_n = \log(1 + b_n/(1 + a_n))$. Based on Proposition 4, it is observed that a_n scales logarithmically with n_t, and hence $\tilde{a}_n$ scales as $\log\log(n_t)$ and $\tilde{b}_n$ vanishes as $n_t \to \infty$. Therefore, the asymptotic average rate (35) in NDR can be approximated as

$$\widetilde{C}_{\mathrm{NDR}} \approx \tilde{a}_n \propto \log\log(n_t), \tag{36}$$

which is in sharp contrast to the rate scaling law (33) obtained for the IPLR.

V. ASYMPTOTIC OUTAGE RATE

In this section, we investigate the SU outage rate in IPLR and NDR. Given a target rate r (nats/s/Hz), the SU rate distribution after transmit antenna selection is defined as the probability that the instantaneous rate $R_{\max}$ is less than r:

$$F_{\mathrm{out}}(r) = \Pr\{R_{\max} < r\}, \tag{37}$$

where $R_{\max}$ is given by (29). The outage rate can be interpreted as the maximum rate, r, such that $F_{\mathrm{out}} \le \epsilon$, where $\epsilon \in (0, 1)$ is the predefined outage threshold. Therefore, the outage rate is expressed as

$$C_\epsilon = \max\{r : F_{\mathrm{out}}(r) \le \epsilon\}. \tag{38}$$

Obtaining the above exact outage rate is algebraically complex. In order to have tractable analysis and gain insight into the considered system, we obtain the asymptotic expressions for the outage rate.

A. OUTAGE RATE IN IPLR

By using the limiting distribution of the SNR in IPLR, the outage rate of the SU is obtained in the following proposition.

Proposition 5: Given the outage probability threshold ϵ in (38), in IPLR, the asymptotic outage rate of the SU with TAS and MRC is expressed by

$$C_\epsilon^{\mathrm{IPLR}} = \log\left[1 + b_n (\log 1/\epsilon)^{-1}\right], \tag{39}$$

where b_n is given in (26).

Proof: Using the limiting distribution (23), and Proposition 3, we obtain the SU asymptotic outage probability.

$$F_{\mathrm{out}}(r) = F_{\gamma_{\max}}\left(e^r - 1\right) = e^{-\frac{b_n}{e^r - 1}}, \tag{40}$$

The proof is completed by inserting (40) into (38). ■

Inserting (32) into (39), the outage rate $C_\epsilon^{\mathrm{IPLR}}$ shows that the SU outage rate scales as $\log(n_t)$ for large n_t in IPLR. The capacity gap between the average rate C_{IPLR} and $C_\epsilon^{\mathrm{IPLR}}$ is calculated as

$$\Delta_c^{\mathrm{IPLR}} = C_{\mathrm{IPLR}} - C_\epsilon^{\mathrm{IPLR}} = \gamma_0 + \log\log(1/\epsilon) + \Delta, \tag{41}$$

where C_{IPLR} is given in (31) and approximated in (33), and

$$\Delta = \log\left(1 + \frac{\log\epsilon}{b_n - \log\epsilon}\right) \propto 1/b_n. \tag{42}$$

As $b_n \propto n_t$, it is obvious that $\Delta < 0$ vanishes at a rate n_t^{-1}. Therefore, given the outage threshold ϵ, the gap between the average rate and the outage rate converges to $\gamma_0 + \log\log(1/\epsilon)$ as $n_t \to \infty$. Hence, $\gamma_0 + \log\log(1/\epsilon)$

TABLE 1. Summary of the asymptotic laws of the outage rate.

Scenario	Asymptotic law	Rate gap[a]
IPLR	$\log(n_t)$	constant gap
NDR	$\log\log(n_t)$	vanishing gap

[a]The difference between the asymptotic values of the average rate and the outage rate.

represents the bound of the rate gap. For instance, given $\epsilon = 10\%$, the rate gap between the outage rate and the average rate is bounded approximately by 1.41125 nats/s/Hz.

B. OUTAGE RATE IN NDR

According to Lemma 3, the asymptotic distribution of $R_{\max}$ can be approximated as (20) with the normalizing coefficients chosen as (34). The SU outage rate in NDR is given in the following proposition.

Proposition 6: With TAS and MRC, the asymptotic outage rate in NDR of the SU is given by

$$C_\epsilon^{\mathrm{NDR}} = \tilde{a}_n - \tilde{b}_n \log\log\left(1/\epsilon\right), \tag{43}$$

where the normalizing coefficients $\tilde{a}_n$ and $\tilde{b}_n$ are given in (34).

Proof: The proof of this proposition is straightforward by substituting (20) into (38). ■

Next, we study the scaling behavior for the SU outage rate in the NDR. From (43) and (35), we can see that the SU outage rate $C_\epsilon^{\mathrm{NDR}}$ scales in the same manner as the SU average rate C_{NDR}. In addition, the capacity gap in NDR, $\Delta_c^{\mathrm{NDR}} = C_{\mathrm{NDR}} - C_\epsilon^{\mathrm{NDR}}$, is given by

$$\Delta_c^{\mathrm{NDR}} = \tilde{b}_n \left[\gamma_0 + \log\log\left(1/\epsilon\right)\right]. \tag{44}$$

where $\tilde{b}_n$ is given in (34), and vanishes as $n_t \to \infty$. Thus, the rate gap between the average rate and the outage rate in NDR diminishes as $n_t \to \infty$.

We summarize the key results of the asymptotic laws of the outage rate in Table 1.

VI. AVERAGE SYMBOL ERROR RATE

In this section we study the average symbol error rate (ASER) for the considered system. Denote SER_i as the symbol error rate when the ith transmit antenna is selected, which is given by

$$\mathrm{SER}_i = \frac{\alpha}{2}\left[1 - \mathrm{erf}\left(\sqrt{\beta\hat{\gamma}_i}\right)\right], \tag{45}$$

where the SNR $\hat{\gamma}_i$ is distributed according to the CDF $F_{\hat{\gamma}_i}(\gamma)$. A generic ASER expression for a wide range of modulation and coding schemes was provided in [51] as

$$\mathrm{ASER} = \min_i \mathbb{E}\left[\mathrm{SER}_i\right] = \mathbb{E}\left[\frac{\alpha}{2}\left(1 - \mathrm{erf}\left(\sqrt{\beta\gamma_{\max}}\right)\right)\right], \tag{46}$$

where α and β are modulation-related parameters, and $\gamma_{\max}$ denotes the maximal SNR $\max_{1\le i\le n_t}(\hat{\gamma}_i)$. As shown in [51], for binary phase-shift keying, $\alpha = 1$ and $\beta = 1$; for binary frequency-shift keying with orthogonal signaling, $\alpha = 1$ and $\beta = 0.5$; for M-ary pulse amplitude modulation, $\alpha = 2(M-1)/M$ and $\beta = 3/(M^2-1)$; and for M-ary phase-shift keying, $\alpha = 2$ and $\beta = \sin^2(\pi/M)$.

By applying the change of variables technique in (45), the CDF of SER_i is given by

$$F_{\mathrm{SER}_i}(x) = 1 - F_{\hat{\gamma}_i}\left(\frac{1}{\beta}\left[\mathrm{erf}^{-1}\left(1 - \frac{2x}{\alpha}\right)\right]^2\right). \tag{47}$$

Based on (46), the average symbol error rate after transmit antenna selection requires the knowledge of the distribution of the minimal symbol error rate among $\{\mathrm{SER}_i\}$, i.e., $\min_{1\le i\le n_t}(\mathrm{SER}_i)$, and eventually the distribution of $\gamma_{\max}$. To the best of our knowledge, it is problematic to obtain the ASER (46) with general modulation and coding schemes using the distribution function $F_{\gamma_{\max}}(x) = \left[F_{\hat{\gamma}_i}(x)\right]^{n_t}$ and (47), where $F_{\hat{\gamma}_i}(x)$ is given in (10). In the following, we present the results achieved by applying EVT.

First, we derive the ASER in IPLR.

Proposition 7: The ASER for the SU of the considered system in IPLR can be approximated as

$$\mathrm{ASER}^{\mathrm{IPLR}} = \frac{\alpha}{2} e^{-2\sqrt{\beta b_n}}, \tag{48}$$

where $b_n = \mu_g \mathrm{S}_Q / \left([n_t/(n_t-1)]^{\zeta/n_r} - 1\right)$ is given in (26).

Proof: By substituting (25) into (46), the symbol error rate can be obtained as

$$ll\mathrm{ASER}^{\mathrm{IPLR}} = \tfrac{\alpha}{2}\int_0^\infty \mathrm{erfc}\left(\sqrt{\beta x}\right) \mathrm{d}e^{-\frac{b_n}{x}} = \tfrac{\alpha}{2} e^{-2\sqrt{\beta b_n}},$$

where in the last step we apply [52, eq. 7.4.20]. ■

This compact result cannot be obtained using $F_{\gamma_{\max}}(x) = \left[F_{\hat{\gamma}_i}(x)\right]^{n_t}$, where $F_{\hat{\gamma}_i}(x)$ is given in (13). Then, using the EVT, we prove in the following proposition that the distribution of the SER (45) in NDR converges to the Weibull distribution, which enables a simple approximation for the ASER of the secondary system with TAS.

Proposition 8: As the number of transmit antenna n_t increases, the distribution of the SER after transmit antenna selection in NDR converges in distribution to the Weibull distribution, given by

$$F_{\mathrm{SER}_{\min}}(x) = 1 - \exp\left[-\left(\frac{2x}{\alpha b_n}\right)^{1/\beta\mu_g S_P}\right] \tag{49}$$

for $0 \le x \le \alpha/2$, and $F_{\mathrm{SER}_{\min}}(x) = 1$ for $x > \alpha/2$, where the normalizing coefficients can be chosen as

$$b_n = a_n - \mathrm{erf}\left(\sqrt{\beta F_{\hat{\gamma}_i}^{-1}\left(1 - 1/n_t\right)}\right). \tag{50}$$

The ASER for the secondary user of the considered system can be approximated as

$$\mathrm{ASER} = \frac{1}{2} b_n\, \beta\, \alpha\, \mu_g S_P\, \gamma\left(\beta\, \mu_g S_P,\ b_n^{-1/\beta\, \mu_g S_P}\right), \tag{51}$$

where b_n is given in (50), and $\gamma(a, x) = \int_0^x e^{-t} t^{a-1} \mathrm{d}t$ is the lower incomplete Gamma function [50, eq. 8.350-1].

Proof: The proof of Proposition 8 is in Appendix E. ■

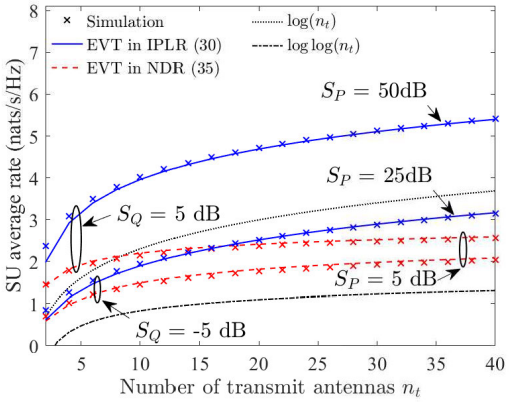

FIGURE 4. SU average rate versus n_t with $n_r = 1$.

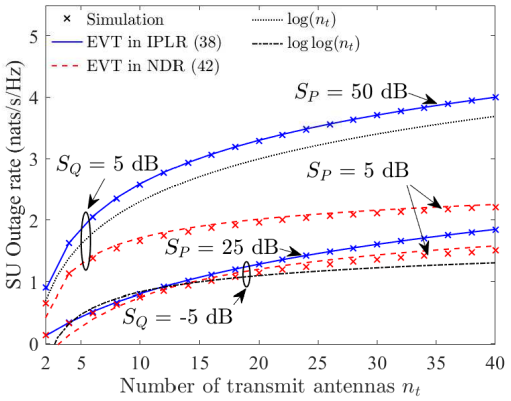

FIGURE 6. SU outage rate versus n_t with $\epsilon = 10\%$ and $n_r = 1$.

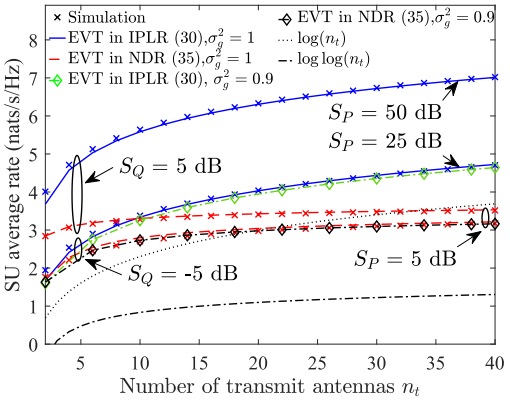

FIGURE 5. SU average rate versus n_t with $n_r = 5$.

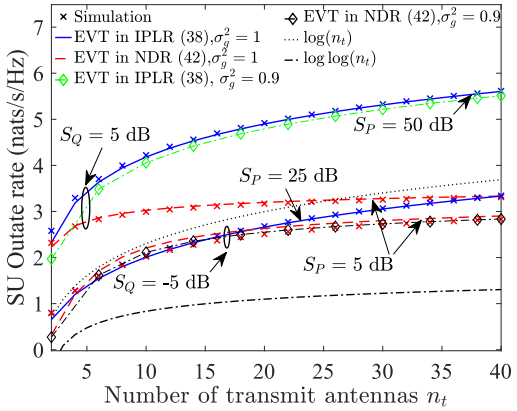

FIGURE 7. SU outage rate versus n_t with $\epsilon = 10\%$ and $n_r = 5$.

VII. SIMULATION RESULTS

This section presents the simulation results of the SU average rate, the outage rate, and the average symbol error rate of the considered system. The ST employs the transmit antenna selection, while the SR employs the maximal ratio combining technique. The transmission of the ST is constrained by the peak interference constraint and the maximal transmit power constraint shown in (4). The average channel gains are set to 1. For each simulated curve, the considered performance metric is averaged over 1×10^6 channel realizations. Under imperfect CSI condition, the channel correlation coefficent between the channel coefficient and the channel estimation is chosen to be 0.9, i.e. $\sigma_g^2 = 0.9$.

Fig. 4 and Fig. 5 depict the average rate of the SU as a function of n_t assuming 1 and 5 receive antennas, respectively. The average rates are plotted for the IPLR and NDR scenarios. We also plot $\log(n_t)$ and $\log\log(n_t)$ to show the corresponding scaling laws. We can see that even for the case with less than 5 transmit antennas the asymptotic results using EVT are quite accurate. We can also observe that the SU average rate scales logarithmically in terms of n_t in IPLR. In NDR, the figures illustrate that the curves of the SU average rate become more flat as predicted by the scaling law in (36), i.e., the average rate scales as $\log(\log(n_t))$. In Fig. 5, the curves with marker $\diamond$ illustrate the average rate for $\delta_g^2 = 0.9$. Compared to the curves of the perfect CSI scenario, they have the same scaling behavior in NDR and IPLR as n_t grows to infinity. This confirms the analysis results in previous sections that the SNR distributions for the perfect and the imperfect scenarios are tail equivalent.

In Fig. 6 and in Fig. 7, we depict the SU outage rate as a function of n_t assuming 1 and 5 receive antennas, respectively. The outage threshold ϵ is set to 10%. The EVT approximations (39) in NDR and (43) in IPLR agree with the simulation results. In addition, the outage rates in each operational regime scale as the number of transmit antenna n_t, following the same scaling law as the corresponding average rate, i.e., in NDR $C_\epsilon \sim \log\log n_t$ and in IPLR $C_\epsilon \sim \log n_t$. In Fig. 7, the curves with marker $\diamond$ show the outage rate for $\delta_g^2 = 0.9$. Compared to the curves of the perfect CSI scenario, they have the same scaling behavior in NDR and IPLR as n_t grows to infinity. This confirms the analysis results for SU outage rate.

Fig. 8 shows the average rate and the outage rate of the SU as a function of the ratio $\rho = S_P/S_Q$ assuming one receive antenna, where $S_P = P_m/\sigma^2$ and $S_Q = Q/\mu_h\sigma^2$. We have the following key observations: (a) the rates approach the IPLR scenario as ρ increases; (b) given n_t, the gap between

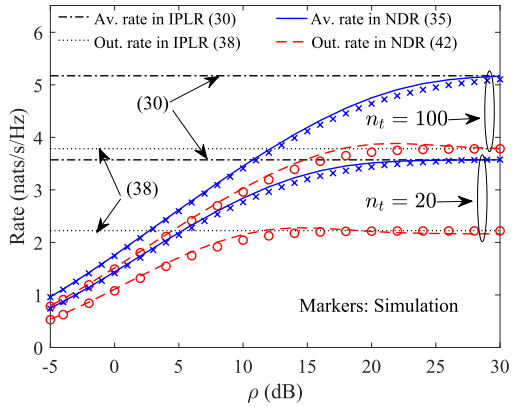

FIGURE 8. SU average rate and outage rate versus $\rho = S_P/S_Q$ with $\epsilon = 10\%$, $S_Q = 0$dB, and $n_r = 1$.

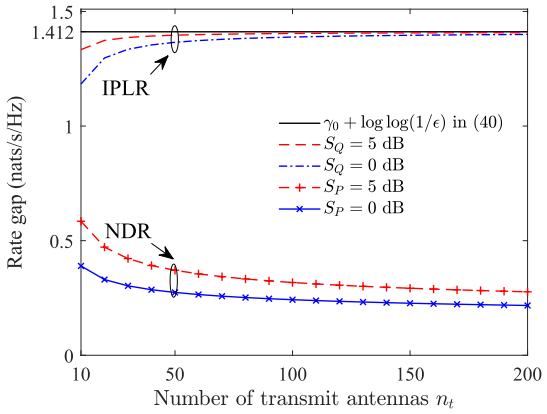

FIGURE 9. Rate gap versus n_t with $n_r = 1$ and $\epsilon = 10\%$. In NDR $S_Q = 0$dB, and $S_P \to \infty$ in IPLR.

the average rate and the corresponding outage rate first increases (NDR regime) and then becomes constant (IPLR regime) as ρ increases; (c) the values of n_t impacts the speed at which the rates transition from NDR to IPLR as ρ increases; for instance, when $n_t = 20$ the outage rate almost saturates at $\rho = 12$, while for $n_t = 100$ the outage rate almost saturates at $\rho = 20$; (d) given n_t, the outage rate approaches to the IPLR scenario faster than the average rate does. These observations confirm that the asymptotic behaviors of the SU rate shift from the NDR regime, governed by Gumbel distribution, to the IPLR regime, governed by the Fréchet distribution, as S_P becomes dominant over S_Q.

The rate gap of the SU between the outage rate and the average rate is depicted in Fig. 9. In addition, we plot the rate ratio for the IPLR and the NDR, which is defined as the ratio of the outage rate and the corresponding average rate. We set $S_P \to \infty$ in IPLR, and $S_Q = 0$dB in NDR. First, the rate gap in IPLR is approaching to a constant value $\gamma_0 + \log\log(1/\epsilon)$ as indicated in (41). Second, the rate gap in NDR is vanishing slowly as suggested by (44). This shows that the average rate can be estimated by the outage rate, which is, in practice, easier to obtain than the average rate in (30).

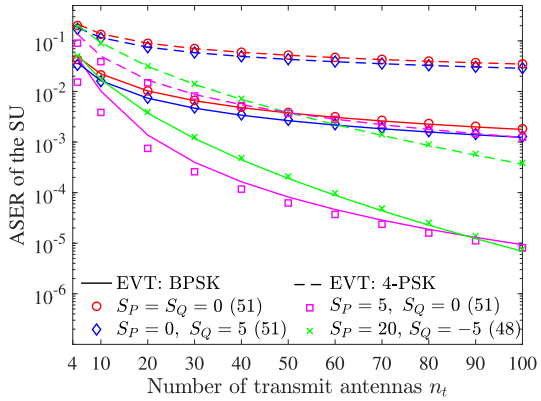

FIGURE 10. SU average symbol error rate versus n_t. The number of receive antennas $n_r = 1$. The markers show the simulation results. The values of S_P and S_Q are in dB.

For instance, given $\epsilon = 10\%$, the rate gap between the outage rate and the average rate is always bounded approximately by 1.41 nats/s/Hz. Moreover, the rate ratio curves confirm these observations.

Fig. 10 shows the SU average symbol error rate for BPSK and 4-PSK modulation schemes as a function of n_t. For the IPLR scenario, we assume that $S_Q = -5$dB and $S_P = 20$dB. The results using EVT in IPLR and NDR are obtained from Proposition 7 and Proposition 8, respectively. For each n_t, the simulation results are obtained by averaging over 10^6 channel realizations. Obviously, the ASER decreases as n_t increases. The figure explicitly illustrates that the ASER curves in IPLR have larger slops than the ones in NDR. Moreover, it shows that when n_t is small the interference power constraint S_Q has more influence on ASER than S_P. Assuming 4-PSK modulation, when $n_t < 50$, the ASER for $S_P = 20$dB and $S_Q = -5$dB has higher value than in the case $S_P = 5$dB and $S_Q = 0$dB. However, when $n_t > 50$, the IPLR provides lower ASER than in NDR. Moreover, the observations clearly illustrate that the ASER as a function of n_t decreases faster in IPLR than that in NDR, which has been predicted in Section VI.

VIII. CONCLUSION

Applying Extreme Value Theory, we revealed a fundamental, yet overlooked property of the SNR distribution of the secondary user in a spectrum-sharing system provided imperfect CSI, where the limiting SNR distributions are governed either by Fréchet or Gumbel distributions. In addition, we showed that the SNR distributions for the perfect and the imperfect scenarios are tail-equivalent. The obtained results enable a compact, yet accurate approximation for the average rate, the outage rate, and the average symbol error rate of the SU for general modulation types. These results, which were overlooked in literature, have been utilized to gain insights into the behavior of the SU average rate, outage rate, and their scaling characteristics in the considered spectrum-sharing system.

Particularly, the SU average rate and outage rate have two scaling behaviors as the number of transmit antennas n_t increases: When the transmit power of the secondary transmitter is mainly restricted by the maximal interference constraint imposed by the primary receiver, i.e. the IPLR regime, the rates of the secondary user scale as $\log(n_t)$; when such interference power constraint is comparable to the maximal transmit power of the secondary transmitter, i.e. the NDR regime, the rates scale as $\log(\log(n_t))$, implying rapidly diminishing gain on adding more antennas. Moreover, the observations of the rate gap between the outage rate and the average rate allows us to estimate the average rate from the corresponding easier-to-obtain outage rate.

APPENDIX A
DERIVATION OF PROPOSITION 1

Let $\mathcal{P}_{\hat{h}} = \Pr\left(|\hat{h}_i|^2 \le \frac{\mathrm{S}_Q}{\mathrm{S}_P}\right) = 1 - e^{-\mathrm{S}_Q/\mathrm{S}_P}$. Recall that $\mathrm{S}_P = P_m/\sigma^2$ and $\mathrm{S}_Q = Q/\mu_h\sigma^2$.

$$
\begin{aligned}
&F_{\hat{\gamma}_i}(x) \\
&= \Pr\left(\min\left\{\frac{\mathrm{S}_Q\|\hat{\mathbf{g}}_i\|_F^2}{|\hat{h}_i|^2}, \mathrm{S}_P\|\hat{\mathbf{g}}_i\|_F^2\right\} \le x\right) \\
&= 1 - \Pr\left(\|\hat{\mathbf{g}}_i\|_F^2 > \frac{|\hat{h}_i|^2\, x}{\mathrm{S}_Q}, \|\hat{\mathbf{g}}_i\|_F^2 > \frac{x}{\mathrm{S}_P}\right) \\
&= 1 - \int_{\frac{\mathrm{S}_Q}{\mathrm{S}_P}}^{\infty} \Pr\left(\|\hat{\mathbf{g}}_i\|_F^2 > \frac{xt}{\mathrm{S}_Q}\right) \mathrm{d}F_{|\hat{h}_i|^2}(t) \\
&\quad - \int_0^{\frac{\mathrm{S}_Q}{\mathrm{S}_P}} \Pr\left(\|\hat{\mathbf{g}}_i\|_F^2 > \frac{x}{\mathrm{S}_P}\right) \mathrm{d}F_{|\hat{h}_i|^2}(t) \\
&= \int_{\frac{\mathrm{S}_Q}{\mathrm{S}_P}}^{\infty} F_{\|\hat{\mathbf{g}}_i\|_F^2}\left(\frac{xt}{\mathrm{S}_Q}\right) \mathrm{d}F_{|\hat{h}_i|^2}(t) + \mathcal{P}_{\hat{h}} F_{\|\hat{\mathbf{g}}_i\|_F^2}\left(\frac{x}{\mathrm{S}_P}\right) \\
&= \sum_{m=1}^{n_r} B_{m-1}^{n_r-1}(\sigma_g^2) \underbrace{\int_{\frac{\mathrm{S}_Q}{\mathrm{S}_P}}^{\infty} \left[1 - \frac{\Gamma\left(m, \frac{xt}{\mu_g \mathrm{S}_Q}\right)}{\Gamma(m)}\right] \mathrm{d}F_{|\hat{h}_i|^2}(t)}_{F_{\hat{\gamma}_i}^{(1)}(x)} \\
&\quad + \mathcal{P}_{\hat{h}} \sum_{m=1}^{n_r} B_{m-1}^{n_r-1}(\sigma_g^2) \left(1 - \frac{\Gamma\left(m, \frac{x}{\mathrm{S}_P\mu_g}\right)}{\Gamma(m)}\right),
\end{aligned}
$$

where

$$
\begin{aligned}
F_{\hat{\gamma}_i}^{(1)}(x) &= \int_{\frac{\mathrm{S}_Q}{\mathrm{S}_P}}^{\infty} \left[1 - \frac{\Gamma\left(m, \frac{xt}{\mu_g \mathrm{S}_Q}\right)}{\Gamma(m)}\right] \mathrm{d}F_{|\hat{h}_i|^2}(t) \\
&= 1 - \left[1 - \frac{\Gamma\left(m, \frac{x}{\mu_g \mathrm{S}_P}\right)}{\Gamma(m)}\right] \mathcal{P}_{\hat{h}} \\
&\quad - \underbrace{\int_{\frac{\mathrm{S}_Q}{\mathrm{S}_P}}^{\infty} F_{|\hat{h}_i|^2}(t) \mathrm{d}\left[1 - \frac{\Gamma\left(m, \frac{xt}{\mu_g \mathrm{S}_Q}\right)}{\Gamma(m)}\right]}_{F_{\hat{\gamma}_i}^{(2)}(x)}
\end{aligned}
$$

with

$$
\begin{aligned}
F_{\hat{\gamma}_i}^{(2)}(x) &= \int_{\frac{\mathrm{S}_Q}{\mathrm{S}_P}}^{\infty} F_{|\hat{h}_i|^2}(t) \mathrm{d}\left[1 - \frac{\Gamma\left(m, \frac{xt}{\mu_g \mathrm{S}_Q}\right)}{\Gamma(m)}\right] \\
&= \frac{1}{\Gamma(m)}\left[\Gamma\left(m, \frac{x}{\mu_g \mathrm{S}_P}\right)\right. \\
&\quad \left. - \left(\frac{x}{\mu_g \mathrm{S}_Q + x}\right)^m \Gamma\left(m, \frac{x}{\mu_g \mathrm{S}_P} + \frac{\mathrm{S}_Q}{\mathrm{S}_P}\right)\right].
\end{aligned}
$$

Hence, $F_{\|\hat{\mathbf{g}}_i\|_F^2}(x)$ given in Proposition 1 is obtained.

APPENDIX B
DERIVATION OF PROPOSITION 2

The distribution functions $F_{\hat{\gamma}_i}(x)$ and $F_{\gamma_i}(x)$ are given in (10) and (11), respectively. We define

$$
\begin{aligned}
\mathcal{U}_k(x) \equiv \frac{1}{\Gamma(k)}&\left[\Gamma\left(k, \frac{x}{\mu_g \mathrm{S}_P}\right)\right. \\
&\left. - \left(\frac{x}{\mu_g \mathrm{S}_Q + x}\right)^k \Gamma\left(k, \frac{x}{\mu_g \mathrm{S}_P} + \frac{\mathrm{S}_Q}{\mathrm{S}_P}\right)\right],
\end{aligned}
$$

where k is an integer and $0 \le \mathcal{U}_k(x) \le 1$. When k is given, $\mathcal{U}_k(x)$ is a decreasing function of x. Therefore, we have $F_{\hat{\gamma}_i}(x) = 1 - \sum_{m=1}^{n_r} B_{m-1}^{n_r-1}(\sigma_g^2)\mathcal{U}_m(x)$ and $F_{\gamma_i}(x) = 1 - \mathcal{U}_{n_r}(x)$. Recall that $\Gamma(k+1) = k\Gamma(k)$, $\Gamma(k, z) = \Gamma(k)e^{-z}\sum_{l=0}^{k-1}\frac{z^l}{l!}$, and $\Gamma(k+1, z) = k\Gamma(k, z) + z^k e^{-z}$. We first prove in (52), as shown at the top of the next page that $\mathcal{U}_k(x)$ is an increasing function of k when other parameters are given.

We verify that

$$
\begin{aligned}
&\lim_{x \to \omega(F_{\gamma_i})} \frac{1 - F_{\hat{\gamma}_i}(x)}{1 - F_{\gamma_i}(x)} \\
&= \lim_{x \to \infty} \frac{\sum_{m=1}^{n_r} B_{m-1}^{n_r-1}(\sigma_g^2)\mathcal{U}_m(x)}{\mathcal{U}_{n_r}(x)} \\
&= \lim_{x \to \infty} \sum_{m=1}^{n_r} B_{m-1}^{n_r-1}(\sigma_g^2) \frac{\mathcal{U}_m(x)}{\mathcal{U}_{n_r}(x)} \\
&\le \lim_{x \to \infty} \sum_{m=1}^{n_r} B_{m-1}^{n_r-1}(\sigma_g^2) \\
&\le (\sigma_g^2)^{n_r-1}
\end{aligned}
$$

This shows that there exists some $0 < \zeta \le (\sigma_g^2)^{n_r-1}$. Hence, according to Definition 1, $F_{\hat{\gamma}_i}(x)$ and $F_{\gamma_i}(x)$ are tail equivalent. Consequently, Proposition 2 holds.

APPENDIX C
DERIVATION OF PROPOSITION 3

As $S_P \to \infty$ or $S_P \gg S_Q$, the c.d.f. is given in (14). Thus, it is easy to verify that

$$
\begin{aligned}
\lim_{t \to \omega(F_{\gamma_i})} \left[\frac{1 - F_{\gamma_i}(tx)}{1 - F_{\gamma_i}(t)}\right] &= \lim_{t \to \infty} \left[\frac{1 - \left(\frac{tx}{tx + \mu_g \mathrm{S}_Q}\right)^{n_r}}{1 - \left(\frac{t}{t + \mu_g \mathrm{S}_Q}\right)^{n_r}}\right] \\
&= \frac{n_r \mu_g \mathrm{S}_Q / (tx) + \mathcal{O}\left(1/t^2\right)}{n_r \mu_g \mathrm{S}_Q / t + \mathcal{O}\left(1/t^2\right)} \\
&= x^{-1},
\end{aligned}
$$

$$\begin{aligned}\mathcal{U}_{k+1}(x) &= \frac{1}{\Gamma(k+1)}\left[\Gamma\left(k+1,\frac{x}{\mu_g \mathrm{S}_P}\right)-\left(\frac{x}{\mu_g \mathrm{S}_Q+x}\right)^{k+1}\Gamma\left(k+1,\frac{x}{\mu_g \mathrm{S}_P}+\frac{\mathrm{S}_Q}{\mathrm{S}_P}\right)\right]\\ &= \frac{1}{\Gamma(k+1)}\left[k\Gamma\left(k,\frac{x}{\mu_g \mathrm{S}_P}\right)+\left(\frac{x}{\mu_g \mathrm{S}_P}\right)^{k}e^{-\frac{x}{\mu_g \mathrm{S}_P}}-\left(\frac{x}{\mu_g \mathrm{S}_Q+x}\right)^{k+1}\left(\frac{x}{\mu_g \mathrm{S}_P}+\frac{\mathrm{S}_Q}{\mathrm{S}_P}\right)^{k}e^{-\frac{x}{\mu_g \mathrm{S}_P}-\frac{\mathrm{S}_Q}{\mathrm{S}_P}}\right.\\ &\quad \left.-k\left(\frac{x}{\mu_g \mathrm{S}_Q+x}\right)^{k+1}\Gamma\left(k,\frac{x}{\mu_g \mathrm{S}_P}+\frac{\mathrm{S}_Q}{\mathrm{S}_P}\right)\right]\\ &= \frac{1}{\Gamma(k+1)}\left[k\Gamma(k)\mathcal{U}_k(x)+k\left(\frac{x}{\mu_g \mathrm{S}_Q+x}\right)^{k}\Gamma\left(k,\frac{x}{\mu_g \mathrm{S}_P}+\frac{\mathrm{S}_Q}{\mathrm{S}_P}\right)+\left(\frac{x}{\mu_g \mathrm{S}_P}\right)^{k}e^{-\frac{x}{\mu_g \mathrm{S}_P}}\right.\\ &\quad \left.-\left(\frac{x}{\mu_g \mathrm{S}_Q+x}\right)\left(\frac{x}{\mu_g \mathrm{S}_P}\right)^{k}e^{-\frac{x}{\mu_g \mathrm{S}_P}-\frac{\mathrm{S}_Q}{\mathrm{S}_P}}-k\left(\frac{x}{\mu_g \mathrm{S}_Q+x}\right)^{k+1}\Gamma\left(k,\frac{x}{\mu_g \mathrm{S}_P}+\frac{\mathrm{S}_Q}{\mathrm{S}_P}\right)\right].\\ \Delta\mathcal{U} &= \mathcal{U}_{k+1}(x)-\mathcal{U}_k(x)\\ &= \frac{1}{\Gamma(k+1)}\left[k\left(\frac{x}{\mu_g \mathrm{S}_Q+x}\right)^{k}\Gamma\left(k,\frac{x}{\mu_g \mathrm{S}_P}+\frac{\mathrm{S}_Q}{\mathrm{S}_P}\right)-k\left(\frac{x}{\mu_g \mathrm{S}_Q+x}\right)^{k+1}\Gamma\left(k,\frac{x}{\mu_g \mathrm{S}_P}+\frac{\mathrm{S}_Q}{\mathrm{S}_P}\right)\right.\\ &\quad \left.+\left(\frac{x}{\mu_g \mathrm{S}_P}\right)^{k}e^{-\frac{x}{\mu_g \mathrm{S}_P}}-\left(\frac{x}{\mu_g \mathrm{S}_Q+x}\right)\left(\frac{x}{\mu_g \mathrm{S}_P}\right)^{k}e^{-\frac{x}{\mu_g \mathrm{S}_P}-\frac{\mathrm{S}_Q}{\mathrm{S}_P}}\right]\geq 0. \end{aligned} \tag{52}$$

where $\mathcal{O}(t^n)$ represents a term of order t^n. Therefore, according to Lemma 2 the distribution $F_{\gamma_i}(x)$ lies on the MDA of Fréchet distribution. Since that $F_{\hat{\gamma}_i}(x)$ and $F_{\gamma_i}(x)$ are tail equivalent as shown in Proposition 2, the distribution $F_{\hat{\gamma}_i}$ lies on the MDA of the Fréchet distribution. This suggests that we can work on an easy tail equivalent distribution and compute the normalizing coefficients for it.

NORMALIZING COEFFICIENTS FOR FRÉCHET

Given the c.d.f. in (14), the corresponding inverse c.d.f. reads

$$F_{\gamma_i}^{-1}(y)=\frac{\mu_g \mathrm{S}_Q}{y^{-1/n_r}-1}. \tag{53}$$

As $x \to \omega(F)$, $F_{\hat{\gamma}_i}(x)$ and $F_{\gamma_i}(x)$ are tail equivalent, i.e., $n_t(1-F_{\hat{\gamma}_i}(b_n x+a_n)) \sim n_t(1-F_{\gamma_i}(b_n x+a_n))\zeta^{-1}$ such that $F_{\hat{\gamma}_i}^{n_t}(b_n x+a_n) \to \left[F_{\gamma_i}^{n_t}(b_n x+a_n)\right]^{\zeta^{-1}}=\left(\frac{x}{x+\mu_g \mathrm{S}_Q}\right)^{n_r/\zeta}$ [44, Proposition 1.19]. Hence, given the c.d.f. in (13), the corresponding inverse c.d.f. can be approximately as

$$F_{\hat{\gamma}_i}^{-1}(y)=\frac{\mu_g \mathrm{S}_Q}{y^{-\zeta/n_r}-1}. \tag{54}$$

Then, using Proposition 3 and (24), the normalizing coefficients (17) for the Fréchet distribution is obtained as

$$a_n=0, \quad b_n=\frac{\mu_g \mathrm{S}_Q}{[n_t/(n_t-1)]^{\zeta/n_r}-1}.$$

Using series expansion to (26) in terms of n_t, we can directly see that $b_n \propto n_t$ as $n_t \to \infty$ given other parameters in (26). This suggests that b_n is unbounded in IPLR.

APPENDIX D
DERIVATION OF PROPOSITION 4

We first show that the distribution $F_{\gamma_i}(x)$ lies on the MDA of the Gumbel distribution, and then apply the property that $F_{\hat{\gamma}_i}(x)$ and $F_{\gamma_i}(x)$ are tail equivalent.

The p.d.f. of γ_i is obtained as the derivative of $F_{\gamma_i}(\cdot)$:

$$f_{\gamma_i}(x)=\frac{e^{-\frac{x\sigma^2}{P_m\mu_g}}x^{n_r-1}}{\Gamma(n_r)}A(x).$$

where

$$\begin{aligned}A(x) &= \left(\frac{\sigma^2}{P_m\mu_g}\right)^{n_r}-\left(\frac{\sigma^2}{P_m\mu_g}\right)\frac{xe^{-\frac{Q}{P_m\mu_h}}}{x+\frac{Q\mu_g}{\mu_h\sigma^2}}\\ &\quad +\frac{n_r Q\mu_g/(\mu_h\sigma^2)}{\left(x+\frac{Q\mu_g}{\mu_h\sigma^2}\right)^{n_r+1}}\Gamma\left(n_r,\frac{x\sigma^2}{P_m\mu_g}+\frac{Q}{P_m\mu_h}\right).\end{aligned} \tag{55}$$

Then we have

$$\frac{f'_{\gamma_i}(x)}{f_{\gamma_i}(x)}=-\frac{\sigma^2}{P_m\mu_g}+\frac{n_r-1}{x}+\frac{A'(x)}{A(x)}, \tag{56}$$

and

$$\lim_{x\to\infty}\frac{A'(x)}{A(x)}=0. \tag{57}$$

Thus,

$$\lim_{x\to\infty}\frac{f_{\gamma_i}(x)}{f'_{\gamma_i}(x)}=-\frac{P_m\mu_g}{\sigma^2}. \tag{58}$$

It is obvious that $\lim_{x\to\infty} f_{\gamma_i}(x)=0$ and $\lim_{x\to\infty}\left[-f'_{\gamma_i}(x)\right]=0$. We need to show, after taking the derivative

according to (19), that

$$\lim_{x\to\infty}\left[\frac{(1-F_{\gamma_i}(x))f'_{\gamma_i}(x)}{f^2_{\gamma_i}(x)}\right]=-1. \tag{59}$$

Since $F_{\gamma_i}(x)$ is the c.d.f. of γ_i, thus we have

$$\lim_{x\to\infty}\left[F_{\gamma_i}(x)-1\right]=0. \tag{60}$$

Therefore we obtain, according to L'Hospital's rule,

$$\begin{aligned}\lim_{x\to\infty}\left[\frac{1-F_{\gamma_i}(x)}{f_{\gamma_i}(x)}\right]&=\lim_{x\to\infty}\left[\frac{\left(1-F_{\gamma_i}(x)\right)'}{f'_{\gamma_i}(x)}\right]\\&=\lim_{x\to\infty}\left[\frac{f_{\gamma_i}(x)}{-f'_{\gamma_i}(x)}\right]=\frac{P_m\mu_g}{\sigma^2}.\end{aligned} \tag{61}$$

First, we assume $P_m < \infty$. Both of the limits $\lim_{x\to\infty}\left[\frac{1-F_{\gamma_i}(x)}{f_{\gamma_i}(x)}\right]$ and $\lim_{x\to\infty}\left[\frac{f_{\gamma_i}(x)}{-f'_{\gamma_i}(x)}\right]$ are finite. Therefore, we have

$$\begin{aligned}&\lim_{x\to\infty}\left[\frac{(1-F_{\gamma_i}(x))f'_{\gamma_i}(x)}{f^2_{\gamma_i}(x)}\right]\\&\quad=\lim_{x\to\infty}\left(\frac{1-F_{\gamma_i}(x)}{f_{\gamma_i}(x)}\right)\lim_{x\to\infty}\left(\frac{f'_{\gamma_i}(x)}{f_{\gamma_i}(x)}\right)=-1,\end{aligned} \tag{62}$$

which indicates that in NDR $F_{\gamma_i}(x)$ is a von Mises function such that it belongs to the MDA of the Gumbel distribution [49]. As a consequence, the distribution $F_{\hat{\gamma}_i}$ also lies on the MDA of the Gumbel distribution since the two distributions are tail equivalent.

NORMALIZING COEFFICIENTS FOR GUMBEL

In NDR, we apply tail equivalence of distribution function to obtain the normalizing coefficients, which provide insights into the scaling laws.

Lemma 4: [53, Proposition 1]. Let F be a common distribution function of i.i.d. random variables X_i, $i = 1,\cdots,N$, which lies on the MDA of Gumbel distribution. Suppose that there exist $\alpha>0$, $\beta\in\mathbb{R}$, $c>0$, and $d>0$ such that

$$\lim_{x\to\infty}\frac{1-F(x)}{\alpha x^\beta e^{-cx^d}}=1.$$

Then, the normalizing coefficients in (17) can be chosen as

$$\begin{aligned}a_n&=(\log(N)/c)^{\frac{1}{d}}\\&\quad+\frac{(\beta/d)\left[\log(\log(N))-\log(c)\right]+\log(\alpha)}{(\log(N)/c)^{1-\frac{1}{d}}\,d\,c},\\b_n&=\frac{(\log(N)/c)^{\frac{1}{d}-1}}{d\,c}.\end{aligned} \tag{63}$$

Proposition 9: In NDR, the asymptotic normalizing coefficients, using the tail equivalence with the common distribution given in (11), can be chosen as

$$\begin{aligned}a_n&=\mu_g\mathrm{S}_P\left[\log(n_t)+(n_r-1)\log(\log(n_t))\right.\\&\quad\left.-\log\Gamma(n_r)+\log(\zeta)+\log\left(1-e^{-\mathrm{S}_Q/\mathrm{S}_P}\right)\right],\\b_n&=\mu_g\mathrm{S}_P,\end{aligned}$$

where, as defined in previous section, $\mathrm{S}_P=P_m/\sigma^2$, and $\mathrm{S}_Q=Q/\mu_h\sigma^2$.

Proof:

$$\begin{aligned}&\lim_{x\to\infty}\frac{1-F_{\hat{\gamma}_i}(x)}{\alpha x^\beta e^{-cx^d}}\\&\quad=\lim_{x\to\infty}\frac{1-F_{\hat{\gamma}_i}(x)}{1-F_{\gamma_i}(x)}\frac{1-F_{\gamma_i}(x)}{\alpha x^\beta e^{-cx^d}}\\&\quad=\zeta\frac{\frac{1}{\Gamma(n_r)}\left(1-e^{-\frac{\mathrm{S}_Q}{\mathrm{S}_P}}\right)\left(\mu_g\mathrm{S}_P\right)^{1-n_r}x^{n_r-1}e^{-\frac{x}{\mu_g\mathrm{S}_P}}}{\alpha x^\beta e^{-cx^d}}.\end{aligned}$$

Applying tail equivalence, we obtain

$$\begin{aligned}&\alpha=\frac{\zeta}{\Gamma(n_r)}\left(1-e^{-\frac{\mathrm{S}_Q}{\mathrm{S}_P}}\right)\left(\mu_g\mathrm{S}_P\right)^{1-n_r},\quad\beta=n_r-1,\\&c=\left(\mu_g\mathrm{S}_P\right)^{-1},\quad d=1,\end{aligned} \tag{64}$$

Then by substituting (64) into (63) and replacing N by n_t, we obtain (28). ∎

Remark: As $S_Q\to\infty$, the considered model is equivalent to the point-to-point TAS/MRC model investigated in [27], and (28) is identical to the results in [27, Lemma 2].

APPENDIX E
DERIVATION OF PROPOSITION 8

We introduce a lemma on the MDA of the Weibull distribution.

Lemma 5: [49, Theorem 1.1.13] Let x^* denote the right end of the random variable X, and $F_X(t)$ be its distribution function. Suppose that x^* is finite, and the first derivative of the distribution $F'_X(t)$ exists for $X<x^*<\infty$. We say that $F_X(t)$ belongs to the MDA of the Weibull distribution, if

$$\lim_{t\to x^*}\frac{(x^*-t)F'_X(t)}{1-F_X(t)}=-\xi^{-1},\quad\xi<0,$$

where ξ is given in (18).

Let $Y_i=\mathrm{erf}\left(\sqrt{\beta\hat{\gamma}_i}\right)$, $\forall i=1,\cdots,n_t$ which are random variables with common distribution function $F_Y(y)$. The c.d.f. $F_Y(y)$, $0<y<1$, can be obtained as

$$\begin{aligned}F_Y(y)&=\Pr\{Y\le y\}=\Pr\left\{\hat{\gamma}_i\le\frac{1}{\beta}\left[\mathrm{erf}^{-1}(y)\right]^2\right\}\\&=F_{\hat{\gamma}_i}\left(\frac{1}{\beta}\left[\mathrm{erf}^{-1}(y)\right]^2\right),\end{aligned}$$

and then

$$F_Y^{-1}(z)=\mathrm{erf}\left(\sqrt{\beta F_{\hat{\gamma}_i}{}^{-1}(z)}\right). \tag{65}$$

Let $H(y)$ denote $\left[\mathrm{erf}^{-1}(y)\right]^2/\beta$ for simplicity, and hence $H(y)\to\infty$ as $y\to1$. Then we have

$$H'(y)=\frac{\mathrm{d}\,H(y)}{\mathrm{d}\,y}=\sqrt{\frac{\pi H(y)}{\beta}}e^{\beta H(y)}.$$

Next we evaluate $\lim_{y\to y^*}(y^*-y)f_Y(y)/(1-F_Y(y))$, where y^* denotes the upper end, i.e., $y^*=1$.

$$\begin{aligned}\lim_{y\to 1}\frac{(1-y)f_Y(y)}{1-F_Y(y)} &= \lim_{y\to 1}\frac{(1-y)f_{\hat{\gamma}_i}(H(y))\,H'(y)}{1-F_{\hat{\gamma}_i}(H(y))}\\ &= \lim_{y\to 1}\frac{\left[1-\mathrm{erf}(\sqrt{\beta H(y)})\right]f_{\hat{\gamma}_i}(H(y))}{1-F_{\hat{\gamma}_i}(H(y))}\sqrt{\frac{\pi H(y)}{\beta}}e^{\beta H(y)}\\ &= \lim_{t\to\infty}\underbrace{\frac{f_{\hat{\gamma}_i}(t)}{1-F_{\hat{\gamma}_i}(t)}}_{C_1}\underbrace{\sqrt{\frac{\pi t}{\beta}}e^{\beta t}\left[1-\mathrm{erf}(\sqrt{\beta t})\right]}_{C_2},\end{aligned}$$

where we replace $H(y)$ by t in the last step, and

$$\begin{aligned}\lim_{t\to\infty}C_1 &= \lim_{t\to\infty}\frac{f_{\hat{\gamma}_i}(t)}{f_{\gamma_i}(t)}\frac{f_{\gamma_i}(t)}{1-F_{\gamma_i}(t)}\frac{1-F_{\gamma_i}(t)}{1-F_{\hat{\gamma}_i}(t)}\\ &= \lim_{t\to\infty}\frac{f_{\gamma_i}(t)}{1-F_{\gamma_i}(t)} = 1/\mu_g S_P.\end{aligned}$$

The last step, we have applied (61) and that $F_{\hat{\gamma}_i}(x)$ and $F_{\gamma_i}(x)$ are tail equivalent. Hence, C_1 has finite limit, i.e. $\lim_{t\to\infty}C_1 = 1/\mu_g S_P$.

Using the identity [52, 7.1.23]

$$1-\mathrm{erf}(x) = \frac{e^{-x^2}}{x\sqrt{\pi}}\left(1-\frac{1}{2x^2}-\cdots\right) \tag{66}$$

for C_2 yields

$$C_2 = \frac{1}{\beta}\left(1-\frac{1}{2\beta t}-\cdots\right).$$

It follows that

$$\lim_{t\to\infty}C_2 = \frac{1}{\beta} < \infty.$$

Consequently, we obtain

$$\lim_{y\to 1}\frac{(1-y)f_Y(y)}{1-F_Y(y)} = \left(\lim_{t\to\infty}C_1\right)\left(\lim_{t\to\infty}C_2\right) = \frac{1}{\beta\mu_g S_P}.$$

Following Lemma 5, we have that $F_Y(y)$ lies in the MDA of the Weibull distribution. In consequence, according to the Fisher-Tippet-Gnedenko theorem given in (18), the limiting distribution of $Z_{n_t}=\max(Y_i,\cdots,Y_{n_t})$ can be written as

$$F_{Z_{n_t}}(z) = \exp\left[-\left(\frac{a_n-z}{b_n}\right)^{1/\beta\mu_g S_P}\right] \tag{67}$$

with the possible normalizing coefficients chosen as

$$a_n = 1 \quad \text{and} \quad b_n = a_n - F_Y^{-1}\left(1-\frac{1}{n_t}\right).$$

Note that error function $\mathrm{erf}(x)$, $\forall x\geq 0$, is invertible and non-decreasing, and hence from (65) b_n reads

$$b_n = 1-F_Y^{-1}\left(1-\frac{1}{n_t}\right) = 1-\mathrm{erf}\left(\sqrt{\beta F_{\hat{\gamma}_i}{}^{-1}\left(1-\frac{1}{n_t}\right)}\right).$$

Recall that $\mathrm{SER}_{\min} = \left[1-\mathrm{erf}\left(\sqrt{\beta\gamma_{\max}}\right)\right]\alpha/2$ defined in Section VI. It follows that $\mathrm{SER}_{\min} = \left(1-Z_{n_t}\right)\alpha/2$. The distribution of $\mathrm{SER}_{\min}$ can be deduced as follows:

$$\begin{aligned}F_{\mathrm{SER}_{\min}}(x) &= 1-F_{Z_{n_t}}(1-2x/\alpha)\\ &= 1-\exp\left[-\left(\frac{2x}{\alpha b_n}\right)^{1/\beta\mu_g S_P}\right]\end{aligned} \tag{68}$$

for $0\leq x\leq \alpha/2$, and $F_{\mathrm{SER}_{\min}}(x)=1$ for $x>\alpha/2$. Substituting (67) into (46) yields the ASER as follows

$$\begin{aligned}\mathrm{ASER} &= \int_0^{\alpha/2}\left[1-F_{\mathrm{SER}_{\min}}(x)\right]\mathrm{d}x\\ &= \int_0^{\alpha/2}\exp\left[-\left(\frac{2x}{\alpha b_n}\right)^{1/\beta\mu_g S_P}\right]\mathrm{d}x\\ &= \frac{1}{2}b_n\,\beta\,\alpha\,\mu_g S_P\,\gamma\left(\beta\,\mu_g S_P,\ b_n^{-1/\beta\,\mu_g S_P}\right),\end{aligned}$$

where in the last step we apply [50, eq. 3.381-8].

REFERENCES

[1] S. Rajendran, B. Van den Bergh, S. Pollin, and T. Vermeulen, "IEEE 5G spectrum sharing challenge: A practical evaluation of learning and feedback," *IEEE Commun. Mag.*, vol. 54, no. 11, pp. 210–216, Nov. 2016.
[2] F. Hu, B. Chen, and K. Zhu, "Full spectrum sharing in cognitive radio networks toward 5G: A survey," *IEEE Access*, vol. 6, pp. 15754–15776, 2018.
[3] R. H. Tehrani, S. Vahid, D. Triantafyllopoulou, H. Lee, and K. Moessner, "Licensed spectrum sharing schemes for mobile operators: A survey and outlook," *IEEE Commun. Surveys Tuts.*, vol. 18, no. 4, pp. 2591–2623, 4th Quart., 2016.
[4] F. Teng, D. Guo, and M. L. Honig, "Sharing of unlicensed spectrum by strategic operators," *IEEE J. Sel. Areas Commun.*, vol. 35, no. 3, pp. 668–679, Mar. 2017.
[5] C. Zhang and W. Zhang, "Spectrum sharing for drone networks," *IEEE J. Sel. Areas Commun.*, vol. 35, no. 1, pp. 136–144, Jan. 2017.
[6] B. Cho, K. Koufos, R. Jäntti, and S.-L. Kim, "Co-primary spectrum sharing for inter-operator device-to-device communication," *IEEE J. Sel. Areas Commun.*, vol. 35, no. 1, pp. 91–105, Jan. 2017.
[7] A. Goldsmith, S. A. Jafar, I. Maric, and S. Srinivasa, "Breaking spectrum gridlock with cognitive radios: An information theoretic perspective," *Proc. IEEE*, vol. 97, no. 5, pp. 894–914, Apr. 2009.
[8] M. E. Tanab and W. Hamouda, "Resource allocation for underlay cognitive radio networks: A survey," *IEEE Commun. Surveys Tuts.*, vol. 19, no. 2, pp. 1249–1276, 2nd Quart., 2017.
[9] N. B. Mehta, S. Kashyap, and A. F. Molisch, "Antenna selection in LTE: From motivation to specification," *IEEE Commun. Mag.*, vol. 50, no. 10, pp. 144–150, Oct. 2012.
[10] S. Asaad, A. M. Rabiei, and R. R. Müller, "Massive MIMO with antenna selection: Fundamental limits and applications," *IEEE Trans. Wireless Commun.*, vol. 17, no. 12, pp. 8502–8516, Dec. 2018.
[11] Y. Yu, H. Chen, Y. Li, Z. Ding, L. Song, and B. Vucetic, "Antenna selection for MIMO nonorthogonal multiple access systems," *IEEE Trans. Veh. Technol.*, vol. 67, no. 4, pp. 3158–3171, Apr. 2018.
[12] S. Sanayei and A. Nosratinia, "Capacity of MIMO channels with antenna selection," *IEEE Trans. Inf. Theory*, vol. 53, no. 11, pp. 4356–4362, Nov. 2007.
[13] A. Bereyhi, S. Asaad, and R. R. Müller, R. F. Schaefer, and A. M. Rabiei, "On robustness of massive MIMO systems against passive eavesdropping under antenna selection," in *Proc. IEEE GLOBECOM*, Dec. 2018, pp. 1–7.
[14] S. Thoen, L. Van der Perre, B. Gyselinckx, and M. Engels, "Performance analysis of combined transmit-SC/receive-MRC," *IEEE Trans. Commun.*, vol. 49, no. 1, pp. 5–8, Jan. 2001.
[15] Z. Chen, J. Yuan, and B. Vucetic, "Analysis of transmit antenna selection/maximal-ratio combining in Rayleigh fading channels," *IEEE Trans. Veh. Technol.*, vol. 54, no. 4, pp. 1312–1321, Jul. 2005.
[16] Z. Chen, Z. Chi, Y. Li, and B. Vucetic, "Error performance of maximal-ratio combining with transmit antenna selection in flat Nakagami-*m* fading channels," *IEEE Trans. Wireless Commun.*, vol. 8, no. 1, pp. 424–431, Jan. 2009.
[17] C.-C. Hung, C.-T. Chiang, N.-Y. Yen, and R.-C. Wu, "Outage probability of multiuser transmit antenna selection/maximal-ratio combining systems over arbitrary Nakagami-*m* fading channels," *IET Commun.*, vol. 4, no. 1, pp. 63–68, Jan. 2010.
[18] V. Blagojevic and P. Ivanis, "Ergodic capacity for TAS/MRC spectrum sharing cognitive radio," *IEEE Commun. Lett.*, vol. 16, no. 3, pp. 321–323, Mar. 2012.

[19] D. Li, "Performance analysis of MRC diversity for cognitive radio systems," *IEEE Trans. Veh. Technol.*, vol. 61, no. 2, pp. 849–853, Feb. 2012.
[20] J.-P. Hong and W. Choi, "Throughput characteristics by multiuser diversity in a cognitive radio system," *IEEE Trans. Signal Process.*, vol. 59, no. 8, pp. 3749–3763, Aug. 2011.
[21] K. Tourki, F. A. Khan, K. A. Qaraqe, H.-C. Yang, and M.-S. Alouini, "Exact performance analysis of MIMO cognitive radio systems using transmit antenna selection," *IEEE J. Sel. Areas Commun.*, vol. 32, no. 3, pp. 425–438, Mar. 2014.
[22] P. L. Yeoh, M. Elkashlan, K. J. Kim, T. Q. Duong, and G. K. Karagiannidis, "Transmit antenna selection in cognitive MIMO relaying with multiple primary transceivers," *IEEE Trans. Veh. Technol.*, vol. 65, no. 1, pp. 483–489, Jan. 2016.
[23] Y. Huang, F. Al-Qahtani, C. Zhong, Q. Wu, J. Wang, and H. Alnuweiri, "Performance analysis of multiuser multiple antenna relaying networks with co-channel interference and feedback delay," *IEEE Trans. Commun.*, vol. 62, no. 1, pp. 59–73, Jan. 2014.
[24] Y. Huang, F. S. Al-Qahtani, C. Zhong, Q. Wu, J. Wang, and H. M. Alnuweiri, "Cognitive MIMO relaying networks with primary user's interference and outdated channel state information," *IEEE Trans. Commun.*, vol. 62, no. 12, pp. 4241–4254, Dec. 2014.
[25] Y. Huang, C. Li, C. Zhong, J. Wang, Y. Cheng, and Q. Wu, "On the capacity of dual-hop multiple antenna AF relaying systems with feedback delay and CCI," *IEEE Commun. Lett.*, vol. 17, no. 6, pp. 1200–1203, Jun. 2013.
[26] Y. Huang, J. Wang, P. Zhang, and Q. Wu, "Performance analysis of energy harvesting multi-antenna relay networks with different antenna selection schemes," *IEEE ACCESS*, vol. 6, pp. 5654–5665, 2018.
[27] D. Bai, P. Mitran, S. S. Ghassemzadeh, R. R. Miller, and V. Tarokh, "Rate of channel hardening of antenna selection diversity schemes and its implication on scheduling," *IEEE Trans. Inf. Theory*, vol. 55, no. 10, pp. 4353–4365, Oct. 2009.
[28] J. Lee, H. Wang, J. G. Andrews, and D. Hong, "Outage probability of cognitive relay networks with interference constraints," *IEEE Trans. Wireless Commun.*, vol. 10, no. 2, pp. 390–395, Feb. 2011.
[29] E. Biglieri, A. J. Goldsmith, L. J. Greenstein, N. B. Mandayam, and H. V. Poor, *Principles of Cognitive Radio*. Cambridge, U.K.: Cambridge Univ. Press, 2012.
[30] Z. Yan, X. Zhang, H.-L. Liu, and Y.-C. Liang, "An efficient transmit power control strategy for underlay spectrum sharing networks with spatially random primary users," *IEEE Trans. Wireless Commun.*, vol. 17, no. 7, pp. 4341–4351, Jul. 2018.
[31] R. Sarvendranath and N. B. Mehta, "Transmit antenna selection for interference-outage constrained underlay CR," *IEEE Trans. Commun.*, vol. 66, no. 9, pp. 3772–3783, Sep. 2018.
[32] R. F. Manna, F. S. Al-Qahtani, and S. A. Zummo, "A full diversity cooperative spectrum sharing scheme for cognitive radio networks," *IEEE Access*, vol. 5, pp. 17722–17732, 2017.
[33] J. M. Peha, "Sharing spectrum through spectrum policy reform and cognitive radio," *Proc. IEEE*, vol. 97, no. 4, pp. 708–719, Apr. 2009.
[34] M. Xia and S. Aissa, "Spectrum-sharing multi-hop cooperative relaying: Performance analysis using extreme value theory," *IEEE Trans. Wireless Commun.*, vol. 13, no. 1, pp. 234–245, Jan. 2014.
[35] H. Ding, J. Ge, D. B. da Costa, and Z. Jiang, "Asymptotic analysis of cooperative diversity systems with relay selection in a spectrum-sharing scenario," *IEEE Trans. Veh. Technol.*, vol. 60, no. 2, pp. 457–472, Feb. 2011.
[36] C. Zhong, T. Ratnarajah, and K.-K. Wong, "Outage analysis of decode-and-forward cognitive dual-hop systems with the interference constraint in Nakagami-*m* fading channels," *IEEE Trans. Veh. Technol.*, vol. 60, no. 6, pp. 2875–2879, Jul. 2011.
[37] L. Musavian and S. Aissa, "Fundamental capacity limits of cognitive radio in fading environments with imperfect channel information," *IEEE Trans. Commun.*, vol. 57, no. 11, pp. 3472–3480, Nov. 2009.
[38] M. Gans, "The effect of Gaussian error in maximal ratio combiners," *IEEE Trans. Commun. Technol.*, vol. COM-19, no. 4, pp. 492–500, Aug. 1971.
[39] J. L. Zhang and G. F. Pan, "Outage analysis of wireless-powered relaying MIMO systems with non-linear energy harvesters and imperfect CSI," *IEEE Access*, vol. 4, pp. 7046–7053, 2016.
[40] D. Lee, "Performance analysis of dual selection with maximal ratio combining over nonidentical imperfect channel estimation," *IEEE Trans. Veh. Technol.*, vol. 67, no. 3, pp. 2819–2823, Mar. 2018.
[41] G. L. Stüber, *Principles of Mobile Communication*, 2nd ed. Norwell, MA, USA: Kluwer, 2001.
[42] J. Proakis and M. Salehi, *Digital Communications*, 5th ed. New York, NY, USA: McGraw-Hill, 2008.
[43] H. A. David and H. N. Nagaraja, *Order Statistics*. Hoboken, NJ, USA: Wiley, 2003.
[44] S. I. Resnick, *Extreme Values, Regular Variation and Point Processes*. New York, NY, USA: Springer-Verlag, 2008.
[45] J. Galambos, *The Asymptotic Theory of Extreme Order Statistics*, 1st ed. New York, NY, USA: Wiley, 1978.
[46] G. Song and Y. Li, "Asymptotic throughput analysis for channel-aware scheduling," *IEEE Trans. Commun.*, vol. 54, no. 10, pp. 1827–1834, Oct. 2006.
[47] Y. Huang and B. D. Rao, "An analytical framework for heterogeneous partial feedback design in heterogeneous multicell OFDMA networks," *IEEE Trans. Signal Process.*, vol. 61, no. 3, pp. 753–769, Feb. 2013.
[48] Z. Zheng, J. Hämäläinen, and Z. Ding, "On the sum rate of fair resource allocation with selective feedback," *IEEE Trans. Wireless Commun.*, vol. 15, no. 8, pp. 5193–5205, Aug. 2016.
[49] L. de Haan and A. Ferreira, *Extreme Value Theory: An Introduction*. New York, NY, USA: Springer, 2006.
[50] I. Gradshteyn and I. M. Ryzhik, *Table of Integrals, Series and Products*, 7th ed. New York, NY, USA: Academic, 2007.
[51] M. R. McKay, A. J. Grant, and I. B. Collings, "Performance analysis of MIMO-MRC in double-correlated Rayleigh environments," *IEEE Trans. Commun.*, vol. 55, no. 3, pp. 497–507, Mar. 2007.
[52] M. Abramowitz and I. A. Stegun, Eds., *Handbook of Mathematical Functions: With Formulas, Graphs, and Mathematical Tables*, 10th ed. New York, NY, USA: Dover, 1972.
[53] R. Takahashi, "Normalizing constants of a distribution which belongs to the domain of attraction of the Gumbel distribution," *Stat. Probab. Lett.*, vol. 5, pp. 197–200, Apr. 1987.

RUIFENG DUAN (S'09–M'14) received the M.Sc. (Tech.) and D.Sc. (Tech.) degrees in telecommunications engineering from the University of Vaasa, Finland, in 2008 and 2014, respectively.

He held a visiting position at the Department of Electrical and Computer Engineering, Prairie View A&M University (a member of the Texas A& M University System). Since August 2014, he has been with the Department of Communications and Networking, Aalto University, Finland. His current research interests include random matrix theory, extreme value theory, ambient backscatter communication, cognitive radio, and ultra-reliable low-latency communications. He was a recipient of the Vaasa University Foundation Scholarship for the academic years of 2010 to 2011 and 2011 to 2012, the Ella and Georg Ehrnrooth Foundation Scholarship, in 2010, the IEEE GLOBECOM 2010 Early-Bird Student Award, and the Best Paper Award at The International Symposium on Networks, Computers and Communications, June 2018.

ZHONG ZHENG (S'10–M'15) received the B.Eng. degree from the Beijing University of Technology, Beijing, China, in 2007, the M.Sc. degree from the Helsinki University of Technology, Espoo, Finland, in 2010, and the D.Sc. degree from Aalto University, Espoo, Finland, in 2015. From 2015 to 2018, he held visiting positions at The University of Texas at Dallas and the National Institute of Standards and Technology. In 2019, he joined the School of Information and Electronics, Beijing Institute of Technology, Beijing, as an Associate Professor. His research interests include massive MIMO, secure communications, millimeter wave communications, random matrix theory, and free probability theory.

RIKU JÄNTTI (M'02–SM'07) received the M.Sc. degree (Hons.) in electrical engineering and the D.Sc. degree (Hons.) in automation and systems technology from the Helsinki University of Technology (TKK), in 1997 and 2001, respectively. In 2006, he joined the Aalto University School of Electrical Engineering, Finland (formerly known as TKK), where he is currently a Full Professor of communications engineering and the Head of the Department of Communications and Networking. Prior to joining Aalto (TKK) in August 2006, he was a Pro-Term Professor with the Department of Computer Science, University of Vaasa. He currently holds docentship at the University of Vaasa. He is an Associate Editor of the IEEE TRANSACTIONS ON VEHICULAR TECHNOLOGY and a Distinguished Lecturer of the IEEE Vehicular Technology Society (Class 2016). His research interests include radio resource control and optimization for machine type communications, cloud-based radio access networks, spectrum and co-existence management, RF Inference, ambient backscatter communication, and quantum communications.

JYRI HÄMÄLÄINEN received the M.Sc. and Ph.D. degrees from the University of Oulu, Finland, in 1992 and 1998, respectively. From 1999 to 2007, he was a Senior Specialist and Program Manager with Nokia, where he worked with various aspects of mobile communication systems and 3GPP standardization. He was nominated to Professor of Aalto University, in 2008, and he was tenured, in 2013. Since 2015, he has been serving as the Dean of the Aalto University School of Electrical Engineering. He has authored or coauthored more than 190 scientific publications and holds more tha 36 US patents or patent applications. His research interests include mobile and wireless systems, special focus being in dynamic and heterogeneous networks, including 4–6G, small cells, multi-antenna transmission and reception techniques, scheduling, relays, and many other topics. He is an Expert Member of the Highest Administrative Court of Finland, nominated by the President of Finland.

ZYGMUNT J. HAAS (S'84–M'88–SM'90–F'07) received the Ph.D. degree in electrical engineering from Stanford University, Stanford, CA, USA, in 1988.

In 1988, he joined the Network Research Area, AT&T Bell Laboratories, where he pursued research in wireless communications, mobility management, fast protocols, optical networks, and optical switching. In 1995, he joined the Faculty with the School of Electrical and Computer Engineering, Cornell University, Ithaca, NY, USA, where he is currently a Professor Emeritus. He is also a Professor and a Distinguished Chair with the Computer Science Department, The University of Texas at Dallas, Richardson, TX, USA, since 2013. He heads the Wireless Network Laboratory, a research group with extensive contributions and international recognition in the area of ad hoc networks and sensor networks. He has authored more than 200 technical conference and journal articles. He holds 18 patents in the areas of wireless networks and wireless communications, optical switching and optical networks, and high-speed networking protocols. His research interests include protocols for mobile and wireless communication and networks, secure communications, and the modeling and performance evaluation of large and complex systems. He was a recipient of the number of awards and distinctions, including best paper awards, the 2012 IEEE ComSoc WTC Recognition Award for outstanding achievements and contribution in the area of wireless communications systems and networks, and the 2016 IEEE ComSoc AHSN Recognition Award for outstanding contributions to securing ad hoc and sensor networks. He has organized several workshops, delivered numerous tutorials at major IEEE and ACM conferences. He served as the Chair for the IEEE Technical Committee on Personal Communications. He served as an Editor for several journals and magazines, including the *IEEE/ACM Transactions on Networking*, the IEEE TRANSACTIONS ON WIRELESS COMMUNICATIONS, the IEEE Communications Magazine, and the Wireless Networks (Springer). He has been a Guest Editor of the IEEE JOURNAL ON SELECTED AREAS IN COMMUNICATIONS ISSUES.